NASA TECHNICAL MEMORANDUM

NASA TM X-1651

NASA TM X-1651

ANALYSIS OF LAUNCH WINDOWS FROM CIRCULAR ORBITS FOR REPRESENTATIVE MARS MISSIONS

by Larry A. Manning, Byron L. Swenson, and Jerry M. Deerwester

NASA Headquarters
Mission Analysis Division
Moffett Field, Calif.

NATIONAL AERONAUTICS AND SPACE ADMINISTRATION • WASHINGTON, D. C. • SEPTEMBER 1968

NASA TM X-1651

ANALYSIS OF LAUNCH WINDOWS FROM CIRCULAR ORBITS FOR REPRESENTATIVE MARS MISSIONS

By Larry A. Manning, Byron L. Swenson,
and Jerry M. Deerwester

NASA Headquarters
Mission Analysis Division
Moffett Field, Calif.

NATIONAL AERONAUTICS AND SPACE ADMINISTRATION

For sale by the Clearinghouse for Federal Scientific and Technical Information
Springfield, Virginia 22151 – CFSTI price $3.00

TABLE OF CONTENTS

ANALYSIS OF LAUNCH WINDOWS FROM CIRCULAR ORBITS FOR REPRESENTATIVE MARS MISSIONS[1]

By Larry A. Manning, Byron L. Swenson,
and Jerry M. Deerwester

NASA Headquarters
Moffett Field, California 94035

SUMMARY

Round-trip missions to Mars have been investigated to define representative launch windows and associated ΔV requirements. The 1982 inbound and the 1986 outbound Venus swingby missions were selected for analysis and serve to demonstrate the influence of the characteristics of the heliocentric trajectories on the launch-window velocity requirement. The analysis investigated the use of optimum one- and two-impulse transfers, plus, a restricted three-impulse transfer employing an intermediate elliptic orbit to transfer from a circular parking orbit to the departure hyperbolic asymptote. Insertion at planet arrival was into an orbit coplanar with the arrival asymptote and any required plane change was performed during the planet departure phase. The study indicates that, with a three-impulse transfer, the ΔV penalty to provide a launch window of 20 days at Earth or 60 days at Mars is no more than 5 to 10 percent above the minimum coplanar requirement. Therefore, use in mission analyses of the coplanar ΔV requirements would not result in large errors if three-impulse transfers are acceptable. However, the results also show that the use of coplanar departure velocity requirements is not a good approximation for these launch windows with one- or two-impulse transfers.

Once the outbound leg and planet orbit have been fixed, the nominal return leg can be reexamined as a function of staytime to minimize the total departure (plane change plus heliocentric) velocity requirement. For the direct return leg, sufficient variation in the plane-change angle can be achieved by varying the leg duration to allow the launch window to be increased for one-impulse transfers. No significant effect occurs for the three-impulse transfers due to their already low ΔV penalties. In the case of the swingby return leg, the swingby requirement so severely restricts the departure vector that no significant variation in the launch window occurs.

The effect of small errors in the second harmonic of the gravitational field of the planet and in the orbit radius are shown to require a continual updating of the orbital parameters while in orbit at the planet. If this is not done, the predicted orbit location can be in error by as much as 5° in longitude after a 50 day staytime.

---

[1]The material in this report was summarized in a paper by the same authors and entitled "Launch Window Analysis for Round Trip Mars Missions," presented at the Canaveral Council of Technical Societies' Fifth Space Congress, Cocoa Beach, Florida, March 11-14, 1968.

INTRODUCTION

Preliminary analysis of interplanetary missions is generally performed with the assumption that launch window penalties can be closely approximated by the change in the coplanar departure velocity requirements throughout the window. Most missions under consideration use a parking orbit prior to departure from either Earth or the planet. This means that a unique orbit inclination exists during the launch period of interest. Since the departure hyperbolic asymptote is time dependent and the orbit plane regresses as a result of planetary oblateness, they will generally be essentially coplanar for only short periods. The rest of the time, an angle will exist between the asymptote direction and the orbit plane. The velocity increment necessary to accomplish the required turning maneuver can be of such magnitude as to render the coplanar assumption invalid.

This report compares three different techniques for performing the turning maneuver from circular orbit during launch windows at both Earth and Mars. These techniques consist of (1) an approximate solution for optimum one-impulse transfer, (2) an iterative solution for optimum two-impulse transfer, and (3) a restricted three-impulse transfer employing an intermediate elliptic orbit from which the required plane change is made. This restricted three-impulse transfer lends itself to a rather simple computer analysis and is not significantly more expensive in terms of ΔV than would be an optimum three-impulse transfer where the required plane change is divided among the three increments. A larger number of impulses can also be used; however, the expected reduction in the propulsive velocity requirement below the three-impulse transfer does not appear to warrant the added operational complexity.

To be meaningful, in terms of spacecraft synthesis, the departure analysis has to be mission oriented. Thus, the impulsive techniques were applied to two specific Mars stopover missions. These two missions encompass the four trajectory legs of interest: direct inbound and outbound and Venus swingby inbound and outbound. Therefore, while the numbers are not directly applicable to other Mars missions, the conclusions can be generalized to other round-trip trajectory modes.

The report is divided into three major sections. In the first section, the orbit transfer techniques which were used are discussed, and parametric data are provided in support of the assumptions and approximations made in the analysis. In the second section the criteria for the mission selection are discussed and the characteristics of the 1982 inbound Venus swingby and of the 1986 outbound Venus swingby which were chosen as representative Mars missions are defined. The coupling of the missions with the transfer techniques is contained in the third section where contour maps of constant velocity increments as functions of inclination and staytime in orbit are presented and discussed. An assessment of the sensitivity of the launch window to trajectory reselection and errors in planet characteristics is also provided in the third section.

METHOD OF ANALYSIS

Orbit Geometry

In considering the launch window problem for a given mission, it is first necessary to establish the variation with time of the relative positions of the orbit plane and the hyperbolic escape asymptote. For the analysis of planetary launch windows, it was assumed that the circular parking orbit at planet arrival was coplanar with the arrival asymptote. The resulting orbit elements are shown in figure 1. A planet-centered right-hand coordinate system with its Z axis at the north pole and its X axis at the planet vernal equinox was chosen as indicated. The arrival asymptote or hyperbolic excess velocity vector is defined conventionally as a planet-centered vector with right ascension, ρ, and declination, δ. The orbit elements of interest, that is, the inclination, i, and longitude of the ascending node, Ω, are related by

$$\sin(\rho - \Omega) = \frac{\tan \delta}{\tan i}$$

for all $i \geq \delta$.

It can be seen that for each inclination there are two orbit planes coplanar with the arrival asymptote. These two orbits can be distinguished by the relative positions of the actual spacecraft approach vector at the time of the final midcourse maneuver, and the planet-centered excess velocity vector. If the spacecraft approaches above the excess velocity vector, it moves toward the north pole of the planet and the magnitude of $\rho - \Omega$ is greater than 90°. This orientation will be referred to as a northern insertion. In the other case, the spacecraft approaches below the excess velocity vector (i.e., toward the south pole) and the magnitude of $\rho - \Omega$ is less than 90°. Figure 1 illustrates this configuration which is called a southern insertion.

The situation at some time after arrival is illustrated by figure 2. The first-order secular perturbation due to planet oblateness causes the orbit plane to regress about the planet in the manner shown. That is, for circular orbits, the inclination of the orbit remains unchanged and the longitude of the ascending node changes by $\Delta\Omega$ (see ref. 1) where

$$\Delta\Omega = -3\pi J_2 \left(\frac{R}{r}\right)^2 (\cos i) N$$

and

$$N = \frac{t}{\tau}\left[1 + \frac{3}{2} J_2 \left(\frac{R}{r}\right)^2 \left(1 - \frac{3}{2}\sin^2 i\right)\right]$$

At that time, the orbit plane makes an angle with the departure asymptote of I_∞. It is this angle that must be compensated for during the departure maneuver.

The orbit geometry at Earth was analyzed in a similar manner except that the initial orbit (corresponding to the orbit at arrvial for the planetary case) was chosen so as to be, through regression, coplanar with the departure asymptote at the nominal departure time; that is, zero plane change was chosen for nominal departure. As with the planetary orbits, two orbital planes exist which satisfy this constraint. These planes are distinguished by the relative location of the actual spacecraft departure and the departure excess velocity vector at the nominal departure date. If the actual departure is above the excess vector, then the spacecraft departure is toward the north pole and the magnitude of $\rho - \Omega$ is greater than 90°. This departure is called a northern injection. The other plane has the spacecraft departing below or south of the excess velocity vector. This departure has a $\rho - \Omega$ less than 90° and is called a southern injection.

Impulsive Analysis

The assumption was made for this analysis that the velocity increments are achieved impulsively. The first effect of this assumption is the neglect of gravity losses. Gravity losses, however, typically are relatively small for these missions and can be approximated or even neglected, as done here, without significant error.

The impulsive assumption greatly simplifies the analysis and is justifiable for the analysis of near coplanar arrivals into and departures from circular orbits. For highly elliptical orbits it is less apparent that for the same velocity increment the orientation between the parking orbit and the escape hyperbola (i.e., planet departure) is preserved whether the velocity is added impulsively or through a finite thrusting time. This orientation is preserved, however, as is shown by the example in figure 3 where the velocity increment required to escape to a hyperbolic excess speed of 6.0 km/sec from Mars is shown as a function of the turning angle, that is, the angle between the line of apsides and the departure asymptote. This example is for a departure from an orbit with an eccentricity of 0.9 and 1000 km periapsis altitude. The initial thrust-to-weight ratio for the finite thrusting maneuver was optimized as a function of the true anomaly at the start of thrusting and, for the propulsion system assumed, varied from about 0.03 near apoapsis to 0.4 near periapsis. It is readily apparent that in the region of interest (i.e., near-periapsis departures where the resulting turning angles are between about 70° and 130°) there is no significant difference between the impulsive and the finite thrusting time velocity increments.

The primary difference between the results for the impulsive thrust and for the finite thrusting time is in the position on the parking orbit at which

the velocity is added. For finite thrusting times, the start of the thrust occurs prior to (i.e., leads) the true anomaly for impulsive velocity addition. That is, to obtain the same excess speed and direction as in the impulsive case, the finite thrusting must be approximately centered about the position of the impulsive velocity addition. Typical lead angles are shown in figure 4. Here the velocity increment to escape to an excess speed of 6.0 km/sec from Mars is shown as a function of true anomaly around an orbit with an eccentricity of 0.9 and a periapsis altitude of 1000 km. The true anomaly shown for the finite thrusting is that at the start of thrusting. It can be seen that for equal velocity increments (and hence approximately equal turning angles), the start of finite thrusting must lead the position for impulsive velocity addition by approximately 5° to 15° in true anomaly for all true anomalies except near apoapsis. Near apoapsis, the associated slow rotation and finite thrust result in a near zero lead-angle requirement. In summary, the assumption of impulsive velocity addition is attractive due to the simplification it permits and appears justified due to the small resultant errors.

Plane-Change Modes

A comparison of three methods of transfer from a circular parking orbit to a hyperbolic asymptote is provided in this paper. These methods are optimal one- and two-impulse direct transfers and a restricted three-impulse transfer that uses an intermediate elliptical orbit. The techniques are described in this section.

The velocity increment calculations require knowledge of the minimum angle, I_∞, between the orbit plane and the departure asymptote. This angle was computed from equation (1) of reference 2, which is reproduced here:

$$\sin I_\infty = \cos i[\sin \delta_b - \tan \delta_a \cos \delta_b \cos(\rho_a - \rho_b - \omega t)]$$

$$\pm(\sin^2 i - \sin^2 \delta_a)^{1/2} \sec \delta_a \cos \delta_b \sin(\rho_a - \rho_b - \omega t)$$

where

ρ	right ascension
i	inclination of parking orbit plane
δ	declination
ω	regression rate
t	time from reference date
$( )_a$	reference vector
$( )_b$	actual departure vector

The reference vector used is the nominal departure vector for Earth launch-window analysis and the arrival vector for Mars launch window analysis.

One-impulse transfers.- The single-impulse transfer problem is one of solving for the minimum velocity increment (ΔV) to achieve the desired departure hyperbolic asymptote from a specified orbit. The exact solution of the minimum impulse results in an expression that does not permit a closed form solution. However, reference 3 contains an approximate solution in terms of the angle I_∞ and of the magnitude of the hyperbolic velocity vector (V_∞). For completeness, the solution is reproduced here:

$$\Delta V/V_c = \left(K^2 + 3 - 2 \left\{ (1 - A) \left[2 + K^2 A + 2K(K^2/4 + A)^{1/2} \right] \right\}^{1/2} \right)^{1/2}$$

where

$$K = V_\infty/V_c$$

$$A = \sin I_\infty$$

and V_c is the circular velocity at orbital altitude

This solution was developed for analyzing departures from a lunar orbit; however, it is general and therefore applicable to planetary analysis. Dimensionless parametric results over the velocity range of interest are shown in figure 5.

Two-impulse transfers.- The two-impulse transfer technique considered in this study utilized one impulse at departure from the circular parking orbit and the second impulse at an "infinite" distance from the planet, that is, at the sphere of influence. The solution used was developed by Gunther in reference 3 and employs an optimal distribution of velocity change and angle change between the two impulses. As with the single-impulse case, the solution was developed for lunar application, but is generally applicable to planetary operation.

The total velocity impulse is computed by the sum of the following equations:

$$\Delta V_1/V_c = \left\{ K_1^2 + 3 - 2 \left[(1 + K_1 W - W^2)(2 + K_1 W) \right]^{1/2} \right\}^{1/2}$$

$$\Delta V_2/V_c = (K^2 - K_1^2 \sin^2 Y)^{1/2} - K_1 \cos Y$$

where

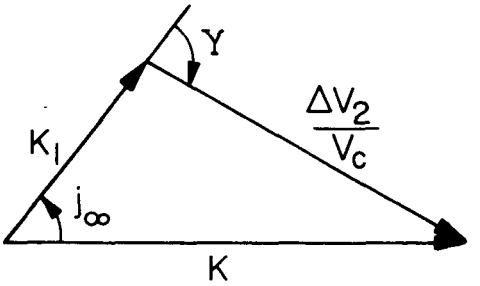

K_1 = $V_{\infty_1}/V_c \equiv$ hyperbolic excess velocity ratio after first impulse

Y $\equiv$ orientation of second impulse (see sketch)

$W = (K^2 + 2)^{1/2} \cos \beta + K$

β = 90° minus flight-path angle of escape hyperbola at orbit intersection

$i_\infty \equiv$ minimum angle between parking orbit plane and K_1

$I_\infty = j_\infty + i_\infty \equiv$ total out-of-plane angle

$$j_\infty = Y - \sin^{-1}\left(\frac{K_1}{K} \sin Y\right)$$

Since the parameters W, Y, and i_∞ are functions of K_1 for optimum transfer, these equations are solved by iteration upon K_1 and give the dimensionless parametric results shown in figure 6. The figure also indicates with a dashed line the boundary beyond which the single impulse solution is optimum.

Three-impulse technique.- The three-impulse mode considered in this study utilizes an in-plane tangential impulse to insert the spacecraft from the circular parking orbit into an intermediate highly elliptical orbit followed by a plane change at apoapsis to rotate the orbit plane so that it is coplanar with the departure asymptote. The motive behind placing the spacecraft into a highly elliptical orbit is to reduce the plane-change velocity requirement by accomplishing the plane-change at apoapsis where the velocity is the lowest. The third impulse is then provided tangentially at the appropriate position on the intermediate ellipse so as to place the spacecraft on the required escape hyperbola. The position of the first impulse on the circular parking orbit is varied parametrically and from these results the optimum position is determined by a numerical search. In general, the optimum position minimizes the plane-change maneuver without an inordinate penalty for an off-periapsis departure from the intermediate ellipse. A complete discussion of this three-impulse technique is given in appendix A.

A brief study was made of off-apoapsis plane-change maneuvers on the intermediate orbit with the motive of rotating the line of apsides in order to reduce off-periapsis departure penalties. It was found that for highly eccentric orbits very little was to be gained, and that the optimum plane-change position was very near apoapsis. This result is primarily a reflection of the low off-periapsis departure penalties for highly elliptic orbits.

The effect of the eccentricity of the intermediate ellipse upon the total departure velocity requirements is shown in figures 7(a) and (b) for Earth and Mars, respectively. These data are for a typical hyperbolic excess speed of 6 km/sec and for an orbit altitude of 1000 km. Curves are shown for various angles, I_∞, between the orbit plane and the departure asymptote. It can be seen, especially for large out-of-plane angles, that high intermediate orbit eccentricities are very attractive.

Parametric data for the three-impulse departure requirements as a function of hyperbolic excess speed are shown in figures 8(a) and (b) for Earth and Mars, respectively. These data are for an orbit altitude of 1000 km and an intermediate orbit with an eccentricity of 0.9. Again, various out-of-plane angles, I_∞, are shown.

MISSION SELECTION CRITERIA

Data to aid in selecting reasonable mission profiles are contained in reference 4 which presents mission characteristics for both direct and Venus swingby stopover missions to Mars for each Earth-Mars opposition period from 1980 to the year 2000. The results of that study indicate that with the exception of the 1984 and 1997 oppositions the swingby mode is more attractive than the direct mode. Propulsive velocity requirements are consistently lower, in some cases affording reductions of 30 percent. Earth entry speeds are also consistently lower, affording reductions of up to 50 percent. These benefits are realized for mission durations of about 500 days, which represents an increase of about 20 percent over the durations for direct missions (based on 30-day stopovers). These mission durations were obtained by minimizing the product of propulsive velocity requirements and mission duration. These "nominal" missions from reference 4 have mission durations about 25 percent shorter than minimum energy missions at the expense of less than a 10-percent increase in total propulsive velocity requirements. As will be demonstrated later, such a mission selection procedure contributes to a low sensitivity of the mission parameters to launch delays. For the above reasons and to encompass typical inbound and outbound swingbys, the launch-window analyses were conducted for the "nominal" mission from reference 4 for the 1982 inbound swingby and for the 1986 outbound swingby.

Since the intent of this paper is to assess the influence of launch delays on mission characteristics, one approach to the selection of the round-trip trajectories could have been the specification of a nominal stopover time. This would have necessitated a further specification on the parking orbit characteristics at Mars to ensure that some other criterion be met, for example, that the nominal departure from Mars be coplanar, or that the plane-change velocity penalty be minimized throughout some arbitrary staytime, etc. The approach taken here is to vary both stopover time and orbit inclination parametrically and to divorce the selection of the outbound leg from the selection of the inbound leg.

Representative Earth departure and Mars arrival conditions must nevertheless be specified. For both mission years considered, the outbound leg chosen is that for the nominal mission employing a 30-day stopover. The Mars departure date was then varied to reflect departure delays. While this may seem restrictive, it is in fact quite reasonable. For outbound swingbys, regardless of mission duration or stopover time, variations of no more than about 10 days arise in either the optimum Earth departure or Mars arrival dates. For inbound swingbys, the variation in Mars arrival date can be on the order of 50 days. However, while the use of the optimum arrival date would reduce

the Mars coplanar departure velocity requirements, it will not significantly influence the plane-change requirements for the various stopover times.

The salient features of the outbound legs for the two missions are contained in table I. It is emphasized that regardless of stopover time the outbound leg characteristics remain fixed as shown.

In order to reduce the sensitivity of Earth departure velocity to delays in Earth departure date, one could, of course, select the outbound leg for any departure date such that the noncoplanar velocity penalty would be minimized. However, this procedure would permit the Mars arrival velocity to be unconstrained. Consequently, the velocity savings at Earth could be more than offset at Mars. In reality, the proper outbound legs can only be chosen when propellant tank volumes and acceptable mass in Earth orbit values are at hand.

This paper is not concerned with system characteristics, yet recognizing that Mars arrival velocities should not be allowed to increase indefinitely, the outbound trajectory legs are selected so that the sums of the Earth departure and Mars arrival velocity increments are equal to the nominal values insofar as possible. When this constant value can no longer be maintained, the trajectories are then selected on the basis of minimizing the velocity sum. Note that this procedure is possible by virtue of the manner by which the nominal missions were defined. If the nominal missions had been selected on the basis of minimum energy, then all delays could cause the velocity requirements to increase.

Figures 9(a) and (b) illustrate the variation of certain outbound leg parameters for the 1982 and 1986 missions, respectively. Notice that in 1982 it is possible to maintain a constant outbound leg velocity requirement (i.e., sum of Earth departure and Mars arrival) for a period of 20 days at Earth departure. Notice that throughout the 40-day window shown, the arrival date at Mars varies by 35 days. In 1986, no variation in the sum of Earth departure and Mars arrival velocities occurs and the Mars arrival date varies by 15 days.

The technique of maintaining constant velocity is also applied successfully to the definition of the inbound legs for launch delays at Mars as shown in figures 10(a) and (b). In this case, only the Mars departure velocity is considered. Constraints could also be imposed on Earth entry speeds, of course, but as can be seen they remain quite low. In 1982, a constant Mars departure velocity can be maintained for all stopover times less than about 50 days. It can be observed also that the variation in inbound leg duration for stopover time up to 100 days at Mars is only 70 days. In 1986, a constant velocity can be maintained for stopover times up to 80 days. Only modest increases in inbound leg duration take place for staytimes up to about 50 days. To maintain either a constant Mars departure velocity or minimum Mars departure velocity for staytimes in excess of about 60 days, it is necessary for the inbound leg heliocentric transfer angle to exceed 180°. Thus, the inbound leg duration must increase accordingly.

NUMERICAL ANALYSIS

In order to provide an assessment of the performance of one-, two-, and three-impulse transfers for representative Mars missions, the techniques described for transfer analysis were applied to the two selected missions. This section presents (1) the results of analyses of the nominal Earth launch window and nominal Mars launch window, (2) the effect of redefining the departure leg at both Earth and Mars, and (3) the sensitivity of the Mars launch-window velocity requirements to orbit radius and planet oblateness uncertainties.

The format selected for presentation of the nominal launch-window data is a contour map, showing lines of constant propulsive velocity requirement on an orbit inclination versus departure date plot. Thus, for a given orbit, the launch window for a given propulsive capability is readily visible. These data are obtained by cross-plotting the complete set of transfer data which is computed for fixed inclinations as a function of departure date. The data necessary to prepare the contour maps are included in appendix B for Earth departures and appendix C for Mars departures.

Earth Launch Window

The launch site considered for these missions was the Kennedy Space Center (KSC). Therefore, the orbit inclinations that can be obtained without a plane change must be between the site's latitude ($\approx 28^\circ$) and the range safety constraint (about 50°). The Earth launch-window analysis was therefore limited to posigrade orbits of 30°, 40°, and 50° inclination.

1982 inbound swingby.- The results for the 1982 launch are shown in figures 11(a) and (b) for a circular orbit of 300 km altitude with an intermediate eccentricity of 0.9 for the three-impulse transfers.

Since the variation of the Earth departure hyperbolic excess velocity for this opportunity is from 4 to 5 km/sec ($K = 0.5 \rightarrow 0.65$), figure 6 indicates that the two-impulse transfer will have lower ΔV requirements than the one impulse for plane-change angles (I_∞) over 15°. Figure 11 shows that the two impulse does indeed lower the ΔV requirement at a given departure date. However, for reasonable velocity penalties associated with the plane change (i.e., 10-20 percent of the minimum coplanar departure ΔV), the increase in launch-window size ($\approx$ 1 day) is not of sufficient magnitude to make the two-impulse transfer of practical interest.

The use of three-impulse transfers is seen to increase the available launch window significantly. For a ΔV of 4.5 km/sec, the three-impulse window is over 24 days for the southern injection (fig. 11(a)). For the same ΔV only a 2-day window is available with a one-impulse transfer. To achieve a 24-day window with the one-impulse transfer would require a ΔV of about 7 km/sec. Thus, the launch-window flexibility provided by a three-impulse transfer makes it worth consideration even with the complexity of performing three maneuvers.

The southern injection orbit rotates relative to the departure vectors such that two coplanar departures occur during the departure period studied. These are indicated by the minimal regions of the figure and are shown graphically in appendix B. Departures between these points require plane changes and thus ΔV penalties. The three-impulse transfer significantly reduces the plane-change ΔV penalty, thus opening this region to low ΔV departures. A comparison of figure 11(a) for the southern injection and figure 11(b) for the northern injection reveals the effect that the orbit direction can have upon the launch window.

For the northern injection (fig. 11(b)), the orbit rotation relative to the departure vector variation results in only one coplanar departure in the departure period studied. A second coplanar departure occurred at an earlier time. As seen in figure 9, this earlier departure has a higher Earth departure ΔV requirement. The plane-change penalty for this orbit orientation is also higher than for the southern injection as seen in appendix B. Therefore, the use of a three-impulse transfer for the northern injection orbit is not as effective as for the southern injection orbit in 1982.

1986 outbound swingby.- The Earth departure data for the 1986 opportunity are shown in figure 12(a) for the southern injection orbit, and in 12(b) for the northern injection. The above conclusions as to the relative value of one-, two-, and three-impulse transfers for the 1982 opportunity apply here as well. The effect of orbit orientation is different, however. For this opportunity, the rotation of northern injection orbit (fig. 12(b)), relative to the departure vectors, allows two coplanar departures over the time period studied. Again, using three-impulse transfer opens the entire departure region between these coplanar points to low ΔV requirements.

Mars Launch Window

The minimum inclination that will allow coplanar arrival and departure is defined by the magnitude of the larger of the declinations at arrival and departure. This inclination is 28.7° and 20.8° for the 1982 and 1986 missions, respectively. The maximum inclination is 180° minus the minimum inclination (i.e., a retrograde orbit). The inclinations were, therefore, varied from 30° to 150° for both missions in 10° intervals.

A circular parking orbit of 1000 km altitude was assumed at Mars. The three-impulse transfer technique again employed an intermediate orbit with an eccentricity of 0.9 to perform the plane-change maneuver. Circular parking orbits allow the coplanar arrival maneuver to be performed tangentially at periapsis of the arrival hyperbola. The insertion ΔV is, therefore, the same for all staytimes, inclinations, and insertion directions. These ΔV are 2.7 and 4.3 km/sec for the 1982 and 1986 Mars arrivals, respectively.

Only contour maps for one- and three-impulse transfers based upon the detailed data of appendix C are shown. The ratio of Mars departure hyperbolic excess velocity to circular velocity at orbit altitude varies from 2 to 4. From figure 6, plane-change angles of 60° or greater must occur before the two-impulse transfer reduces the ΔV penalty below that of the one-impulse

transfer. Since such plane-change angles rarely occurred for the 1982 mission, the two-impulse data are not shown for Mars departure. The velocity ratio for the 1986 mission is about 1.2 which requires a plane-change angle of over 45° for the two impulse to be better than the one impulse. Plane changes of that magnitude occurred for inclinations of 60° to 120°; however, the reduction in ΔV achieved through use of the two-impulse transfer was small compared to the total ΔV requirement and is not shown.

1982 inbound swingby.- Figures 13(a) through (d) present the contour maps of the ΔV requirements for the 1982 mission. The figures show the data for the southern insertion with one and with three impulses and the northern insertion with one and with three impulses.

Figure 13(a) shows that for a one-impulse escape from a southern insertion orbit, three distinct regions exist for a low ΔV capability. These are a nearly polar orbit for staytimes up to 50 days and both low inclination posigrade and high inclination retrograde orbits at 50 days staytime, plus or minus 10 days. In order to provide continuous departure capability up to about 80 days for all available inclinations, a ΔV of 9 km/sec is required. The low ΔV region near 90° inclination occurs since the arrival and departure right ascensions are nearly the same for about 60 days staytime.

Three-impulse transfers from a southern insertion orbit (fig. 13(b)) permit use of low inclinations for short staytimes (5 days) with a low ΔV (5 km/sec) capability. When the ΔV capability is increased to 6 km/sec, all inclinations obtainable can be achieved for staytimes up to 70 days. This is a significant improvement over the one-impulse transfer. A similar increase in staytimes available does not occur by increasing the ΔV from 6 to 7 km/sec since the coplanar velocity requirement rises rapidly after 60 days staytime (fig. 10(a)).

For this 1982 mission, using a northern insertion at arrival increases the launch window for a low to moderate ΔV capability. This is shown in figures 13(c) and (d). The northern insertion direction effectively shifts the ΔV curves forward 20 days as can be seen from a comparison of figures 13(a) and (c). This orbital configuration allows a ΔV of 6 km/sec with a one-impulse transfer to provide staytimes for all inclinations of up to 40 days and for some inclinations of up to 70 days. The three-impulse transfer provides basically the same launch-window capability for either orbit insertion since the plane-change penalty is minimal.

1986 outbound swingby.- The data for the 1986 Mars launch windows are presented in figures 14(a) through (d). Between 60 and 70 days staytime a discontinuity occurs in the return leg characteristics. This results from the trajectory selection since the central angle of the transfer conic crosses the 180° ridge. Solutions can, of course, be found in this region if a finer grid of staytimes is used than was done here, or by constraining the central angle.

Figure 14(a) shows the data for a southern insertion with a single-impulse departure. The data does not display the symmetry about 90°

inclination shown by the 1982 mission since the arrival and departure right ascensions are at least 45° apart for the first 60 days of staytime. After 60 days, the symmetry is stronger. For low total ΔV capability (10 to 20 percent above minimum coplanar ΔV requirement) only small strips of the inclination-staytime map are available. A ΔV of 4 km/sec opens the low inclination region for staytimes to about 80 days. However, to achieve polar orbits for this mission would require a ΔV of about 5 km/sec if only a one-impulse transfer were to be used.

Comparison of these data to figure 14(b) for the southern insertion with a three-impulse transfer reveals the effect of reducing the plane-change penalty. With a three-impulse transfer, a ΔV of about 3.1 km/sec will allow use of all available inclinations for the staytimes shown.

The effect of using a northern insertion at arrival for the 1986 mission is shown in figures 14(c) and (d). For this opportunity, the shift in data, mentioned for 1982, is only about 10 days and does not significantly change the region available for a given ΔV level. A ΔV of 5 km/sec is required for either insertion to provide a reasonably large inclination-staytime spectrum for single-impulse transfers. The effect of the different insertion upon the three-impulse data is negligible with a ΔV of about 3.1 km/sec required to open the entire region of inclinations and staytimes studied.

Mission Profile Reselection

The preceding discussion has presented data that allow the definition of Earth and Mars launch windows. That analysis was based upon the assumed nominal trajectory legs as defined by the mission selection criteria. Using different criteria in the selection of the mission profile could possibly result in more nearly coplanar departures and, therefore, larger launch windows without increasing the velocity penalty for the one-impulse transfers. This possibility was investigated for both the direct return leg and the Venus swingby outbound leg of the 1986 mission. The results are described in this section.

Two constraints were placed upon the reselected mission profile. First, the outbound leg and the return leg were reselected separately. No interaction effects of the reselection were considered even though, if a specific staytime were desired, the reselected outbound leg could influence the selection of the return leg. Second, the total ΔV was not allowed to be less than the minimum coplanar ΔV for the nominal missions. This was done so that a fair comparison could be made to the nominal missions since many of the nominals would have a lower total ΔV if a different criterion had been employed in the original selection.

Reselection of direct inbound leg.- An orbit inclination of 60° was used for the analysis since it has relatively high ΔV penalties and is in the region of interest from a planetary operations standpoint. The total departure velocity increment versus staytime, resulting from the reselection of the direct return leg of the 1986 mission, is shown in figure 15 as dashed lines for both northern and southern orbital insertions. The velocity

requirements for the nominal return legs are reproduced from appendix C as solid lines in the figure to allow a direct comparison of the one-impulse transfers. The characteristics of the reselected return leg vary significantly with staytime as influenced by the orientation of the orbit at any given date. The Earth entry velocity varies between 12 and 14 km/sec and return leg durations vary between 135 and 280 days. This latter value is only 40 days greater than the maximum duration for the nominal missions.

It can be seen that reselecting the direct return leg does indeed reduce the plane-change penalty for the staytimes considered. In fact, if the maximum ΔV is 3.1 km/sec as for the three-impulse transfer previously discussed, a launch window of 33 days will exist for the one-impulse transfer. A ΔV capability of only 3.3 km/sec would allow a 60-day window, the equal of the three-impulse transfer, without the need for restarting the departure engine or the weight penalty for use of several engines.

From the results of this analysis it is concluded that sufficient flexibility of direct leg duration exists to allow relatively low single-impulse penalties for launch windows of 30 to 60 days. Thus, the selection of the orbit inclination can be considered primarily from the operation standpoint for both one- and three-impulse transfers without extreme penalties for reasonable launch windows.

Reselection of Venus swingby leg.- A Venus swingby trajectory, used for the outbound leg of the 1986 mission, has the characteristic that for a fixed Earth departure date only a small range of Venus swingby dates allows successful Mars intercepts. Consequently, the right ascension and the declination of the Earth departure vector are essentially constant. It is therefore concluded that no significant changes in the one-impulse velocity requirements are to be found by reselecting the swingby leg of the mission. Since geometric considerations are similar, this conclusion should be applicable to the swingby leg of any other mission.

Sensitivity of Velocity Requirements

The previous sections have discussed the effect of orbit inclination, staytime, and trajectory selection upon the velocity requirements for planet departures. This section considers the effect of uncertainties in the orbital radius and planet J_2 term on circular orbits. The principal effect in both cases is to change the regression rate of the orbit. The regression rate in turn influences the frequency with which the departure vector lies in the orbit plane, and thus the ΔV requirement at a given time.

The ΔV data for orbital altitudes of 300 and 1000 km are shown in figure 16 for the nominal 1986 return leg with an orbit inclination of 60° for the single-impulse transfer. The 1000 km altitude used for the main portion of the study has one coplanar departure opportunity during the first 60 days of staytime. The 300 km altitude creates a higher regression rate and provides two coplanar departure opportunities during the same interval, while retaining about the same maximum ΔV requirement. This reduces the duration of any given window if less than the maximum velocity requirement is available

A similar effect will occur for even small errors in the orbit radius. A 25-km error in the radius of the orbit (0.07 percent) results in an error of 2 percent in the orbital period for a fixed altitude. With this error, a staytime of only 50 days would result in the location of the ascending node being in error by about 5° (i.e., 1 day), thus affecting the predicted date of coplanar departure and the magnitude of the plane change for noncoplanar departures. This effect is, of course, much more significant for the one-impulse transfer, where a change in I_{∞} of 5° represents as much as 0.3 km/sec ΔV penalty, than for the three-impulse transfer where the ΔV penalty is an order of magnitude less.

The change in the predicted longitude of the ascending node due to an uncertainty in J_2 can be determined by taking a derivative of the equation for $\Delta\Omega$ on page 3. A 5-percent error in J_2 for the orbit altitude studied would result in an error in Ω defined by

$$\delta\Omega = 0.32t \cos i \text{ (deg)}$$

For a 50 day staytime and an inclination of 60°, the error in the predicted location of the ascending node would be 8°.

It should be pointed out that these are long-term prediction errors. Operationally, continual updating of the orbital data will allow reasonably accurate prediction of the orbit parameters at the time of departure.

CONCLUSIONS

The data presented in this report show that, in general, the use of coplanar velocity requirements does not accommodate reasonably launch-window penalties for either one- or two-impulse transfers. Providing a departure ΔV capability for one-impulse transfers on any day during a launch window of 20 days at Earth or 60 days at Mars can result in penalties that are 50 percent of the nominal coplanar departure ΔV requirement. Two-impulse transfers, while reducing the peak velocity penalty, do not significantly increase the launch windows associated with one-impulse transfers for reasonable ΔV penalties. However, use of three-impulse transfers from circular orbits permits the same launch windows, 20 days at Earth and 60 days at Mars, for ΔV penalties on the order of 10 percent of the coplanar departure ΔV requirement.

The orbit precession as determined by the direction of injection (Earth) or insertion (Mars) can significantly affect the launch-window duration. One direction results in a precession which follows the departure vector and thus reduces the plane-change penalty. This effect was more pronounced at Earth than at Mars.

The analysis has revealed that if the parking orbit inclination and direction are fixed, the proper selection of the departure leg, for direct transfers between the planets, can produce launch windows with acceptable ΔV penalties for one-impulse transfers. Since the orbit is fixed, its motion as

a function of staytime is known and the departure trajectory which minimizes the total departure ΔV (i.e., the ΔV that includes both plane change and velocity increase) can be found. This conclusion is generally not applicable to Venus swingby legs since the swingby requirement severely restricts the departure vector variations.

Small errors (<5 percent) in the knowledge of the orbital radius and of the J_2 term can cause errors of 5° in the predicted location of the orbital ascending node for staytimes of 50 days. While this error does not significantly change the magnitude of the maximum ΔV requirement, the ΔV requirement for a particular staytime can change by as much as 0.3 km/sec for a one-impulse transfer. These errors can be reduced through updating of the orbital parameters during the stopover.

National Aeronautics and Space Administration
Moffett Field, Calif., 94035, Sept. 18, 1967
130-06-04-01-15

APPENDIX A

THREE-IMPULSE ANALYSIS

Figure 17 indicates the geometry and notation used in the analysis of the restricted three-impulse escape maneuver. At the time of departure, the circular parking orbit plane is specified by the longitude of the ascending node (measured from the planet's vernal equinox), Ω, and the inclination, i. The departure asymptote is specified by two angles; the right ascension, ρ, and declination, δ. The first impulse to insert the spacecraft into the intermediate ellipse is applied at an angle ω measured in the orbital plane from the ascending node. Since the impulse is applied tangentially, this position becomes the periapsis of the intermediate ellipse and is designated by the unit vector $\hat{r}_p$. The orbit plane is then rotated with the second impulse at apoapsis of the intermediate ellipse (i.e., at $-\hat{r}_p$) so as to be coplanar with the departure asymptote, $\hat{V}_\infty$.

The third or escape impulse is applied tangentially at an appropriate point on the intermediate ellipse (see fig. 18) such that the correct escape asymptote direction and speed are achieved. Using a tangential impulse to escape from the intermediate ellipse greatly simplifies the calculation of the escape maneuver and sacrifices very little in ΔV accuracy over the optimal single-impulse escape where flight-path angle is changed. This is illustrated in figures 19 and 20 which show the velocity increment required to escape from Mars to a velocity at infinity of 6 km/sec coplanar from orbits with eccentricities equal to 0.6 and 0.9, respectively. The velocity increments are shown as a function of turning angle, P, and results are shown for both optimum single-impulse and tangential single-impulse escape maneuvers. It can be seen for near-periapsis departures (i.e., P near 100° in this case) that the tangential single impulse approximates the optimum single impulse to within 0.1 km/sec for 90° either side of periapsis, thus justifying this considerable simplification.

The departure point on the ellipse in figure 18 is designated by the true anomaly, θ_e, and also by the true anomaly on the escape hyperbola, θ_h. The key independent parameter is the angle between the periapsis unit vector, $\hat{r}_p$, and the departure asymptote unit vector $\hat{V}_\infty$, and is designated as P. It is convenient to invert the escape problem and the roles of dependent and independent parameters by specifying θ_e and then determining the resulting angle P.

Applying the conditions of tangency between the escape hyperbola and the intermediate ellipse at the point where ΔV_3 is applied and then solving for the unknown eccentricity of the hyperbola yields:

$$e_h = \left[1 - \left(\frac{r}{a}\right)\left(\frac{2 - r/a}{1 + \tan^2 \gamma}\right)\right]^{1/2}$$

where

$$r = \frac{r_p(1 + e_e)}{1 + e_e \cos \theta_e}$$

$$a = - \frac{\mu}{V_\infty^2}$$

and

$$\tan \gamma = \frac{e_e \sin \theta_e}{1 + e_e \sin \theta_e}$$

The true anomaly on the escape hyperbola is then given by

$$\sin \theta_h = \frac{1 - e_h^2}{e_h} \frac{\tan \gamma}{r/a}$$

$$\cos \theta_h = \frac{1}{e_h} \left(\frac{1 - e_h^2}{r/a} - 1 \right)$$

In figure 18, the asymptote half-angle, ϵ, is determined by

$$\epsilon = \cos^{-1} \frac{1}{e_h}$$

and the angle P is finally determined by

$$P = \pi - \epsilon + \theta_e - \theta_h$$

The third velocity increment, ΔV_3, is given directly by

$$\Delta V_3 = \left(\mu \frac{2}{r} + V_\infty^2 \right)^{1/2} - \left[\mu \left(\frac{2}{r} - \frac{1 - e_e}{r_p} \right) \right]^{1/2}$$

The unit vector normal to the original orbit plane, $\hat{n}$, in figure 17, is given by

$$\hat{n} = \sin \Omega \sin i \, \hat{i} - \cos \Omega \sin i \, \hat{j} + \cos i \, \hat{k}$$

The unit vector, $\hat{r}_p$, is then simply determined by

$$\hat{r}_n \times \hat{r}_p = \sin \omega \, \hat{n}$$

and

$$\hat{r}_n \cdot \hat{r}_p = \cos \omega$$

where $\hat{r}_n$ is the unit vector at the ascending node and is given by

$$\hat{r}_n = \cos \Omega \, \hat{i} + \sin \Omega \, \hat{j}$$

The unit vector in the direction of the departure asymptote is given by

$$\hat{V}_\infty = \cos \delta \cos \rho \, \hat{i} + \cos \delta \sin \rho \, \hat{j} + \sin \delta \, \hat{k}$$

and the angle P is then determined from

$$\cos P = \hat{r}_p \cdot \hat{V}_\infty$$

The unit vector normal to the departure orbit plane (see fig. 18) is then given by

$$\hat{n}_e = \frac{\hat{r}_p \times V_\infty}{\sin P}$$

and thus the plane-change angle required at apoapsis to rotate the original orbit plane coplanar with $\hat{V}_\infty$ is given simply by

$$\cos \Delta = \hat{n}_e \cdot \hat{n}$$

The required velocity increment is

$$\Delta V_2 = 2\left\{\frac{\mu}{r_p}\left[2\left(\frac{1 + e_e}{1 - e_e}\right) - (1 - e_e)\right]\right\}^{1/2} \sin \frac{\Delta}{2}$$

The first velocity increment is, of course, determined by

$$\Delta V_1 = \left(\frac{\mu}{r_p}\right)^{1/2} \left[(1 + e_e)^{1/2} - 1\right]$$

and total escape velocity requirement is thus given by

$$\Delta V = \Delta V_1 + \Delta V_2 + \Delta V_3$$

APPENDIX B

EARTH DEPARTURE REQUIREMENTS

The data presented within this appendix show the total ΔV required for Earth departure versus departure date for each inclination considered. Figures 21(a-c) present the data for the 1982 inbound swingby at inclinations of 30°, 40°, and 50°, respectively. Figures 22(a-c) present similar data for the 1986 outbound swingby. The velocity requirements for one, two, and three impulses are shown in each figure for both southern and northern injections into the outbound interplanetary leg. Also shown is the coplanar departure ΔV for each departure data.

For the departure analysis, the orbital plane was assumed coplanar with the nominal departure vector. This was defined for the departure dates of 244 4990 and 244 6160 for the 1982 and 1986 opportunities, respectively. Thus, all inclinations have no plane-change requirement for the nominal departure. Because of the orbit regression, each combination of inclination and orbit orientation (injection direction) will have other coplanar dates, with a finite plane-change requirement for all noncoplanar dates.

Cross plots of these data at fixed values of ΔV resulted in figures 11 and 12. The reduction of the maximum ΔV requirement achieved when a two-impulse transfer was used instead of a one-impulse transfer is evident for each inclination. It can also be seen that the small difference between the one- and two-impulse transfers at low ΔV (i.e., 10 to 20 percent above minimum coplanar) is due to the steep slope of the curves near the coplanar dates. The success of the three-impulse transfer in reducing the plane-change penalty is evident in all figures.

APPENDIX C

MARS DEPARTURE REQUIREMENTS

The data in this appendix present the total ΔV requirement as a function of staytime for departures from a circular orbit at Mars. Inclinations from 30° to 150° in 10° increments are shown for the 1982 mission in figures 23(a-m) and for the 1986 mission in figures 24(a-m), respectively. Data are included for one-impulse and three-impulse transfers with both north and south orbital insertions. The coplanar departure ΔV of figure 10 is repeated in figures 24 but not in figures 23 to avoid confusion with the three-impulse data. As mentioned in the text, the discontinuity around 65 days staytime for the 1986 mission results from the central angle of the interplanetary transfer leg crossing the 180° ridge.

The orbit is initially positioned by a coplanar arrival for the nominal mission. Staytime was then varied from zero to 100 days staytime in 10-day increments. The nominal arrival dates at Mars are 244 5210 and 244 6500 for the 1982 and 1986 missions, respectively.

Cross plots of these data resulted in figures 13 and 14.

APPENDIX D

NOTATION

a	semimajor axis, km
e	eccentricity
H	altitude, km
I_∞	minimum angle between departure vector and orbit plane, deg
i	inclination, deg
J_2	second harmonic of planetary oblateness
K	ratio of excess velocity to circular velocity
n	normal vector
P	turning angle, deg
R	planet radius, km
r	orbit radius, km
t	time, sec
V_∞	hyperbolic excess velocity, km/sec
V	velocity relative to planet, km/sec
ΔV	propulsive velocity increment, km/sec
x,y,z	components of the planet-centered coordinate system
γ	flight-path angle, deg
Δ	plane-change angle at apoapsis for three-impulse transfer, deg
δ	declination, deg
ϵ	asymptote half-angle, deg
θ	true anomaly, deg
μ	gravitational parameter, km^3/sec^2
ρ	right ascension, deg

τ	unperturbed orbital period, sec
γ	orientation of second impulse in two-impulse transfer
ϕ	central angle of interplanetary leg, deg
Ω	longitude of ascending node, deg
ω	orbital regression rate, deg/sec; also, for appendix A, as defined in figure 17, deg
$(\hat{})$	unit vector

Subscripts

a	reference data
b	departure data
c	circular
e	ellipse
h	hyperbola
i	intermediate ellipse for three-impulse transfer
n	node
p	periapsis
$\varphi,\oplus,\sigma$	Venus, Earth, and Mars
1,2,3	first, second, and third impulse

REFERENCES

1. Roy, Archie E.: The Foundations of Astrodynamics. The Macmillan Company, 1965, p. 224.

2. Deerwester, J. M.; McLaughlin, J. F.; and Wolfe, J. F.: Earth-Departure Plane Change and Launch Window Considerations for Interplanetary Missions. J. Spacecraft Rockets, vol. 3, no. 2, Feb. 1966, pp. 169-174.

3. Gunther, P : Asymptotically Optimum Two-Impulse Transfer from Lunar Orbit. AIAA J., vol. 4, no. 2, Feb. 1966, pp. 346-352.

4. Deerwester, J. M.; and D'Haem, S. M.: Systematic Comparison of Venus Swingby Mode With Standard Mode of Mars Round Trips. J. Spacecraft Rockets, vol. 4, no. 7, July 1967, pp. 904-911.

TABLE I.- NOMINAL OUTBOUND LEG CHARACTERISTICS

Opp. Year	Leave Earth					Pass Venus		Arrive Mars				
	Date*	V_∞ (EMOS)	ΔV, km/sec	ρ, deg	δ, deg	Date*	r_p/R_φ	Date*	V_∞	ΔV	ρ	δ
1982	4990	0.555	4.11	145.4	-0.6	---	---	5210	0.125	2.70	288.1	-4.4
1986	6160	.154	4.10	74.5	19.9	6317	1.76	6500	.200	4.28	285.0	-20.8

*All dates are Julian minus 244 0000

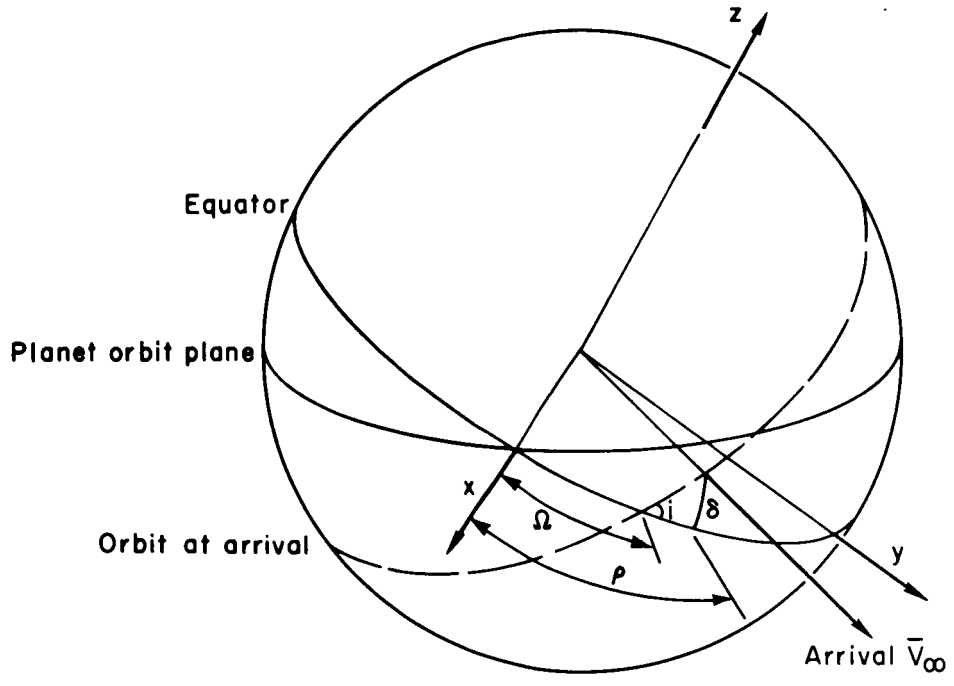

Figure 1.- Orbit geometry at planet arrival.

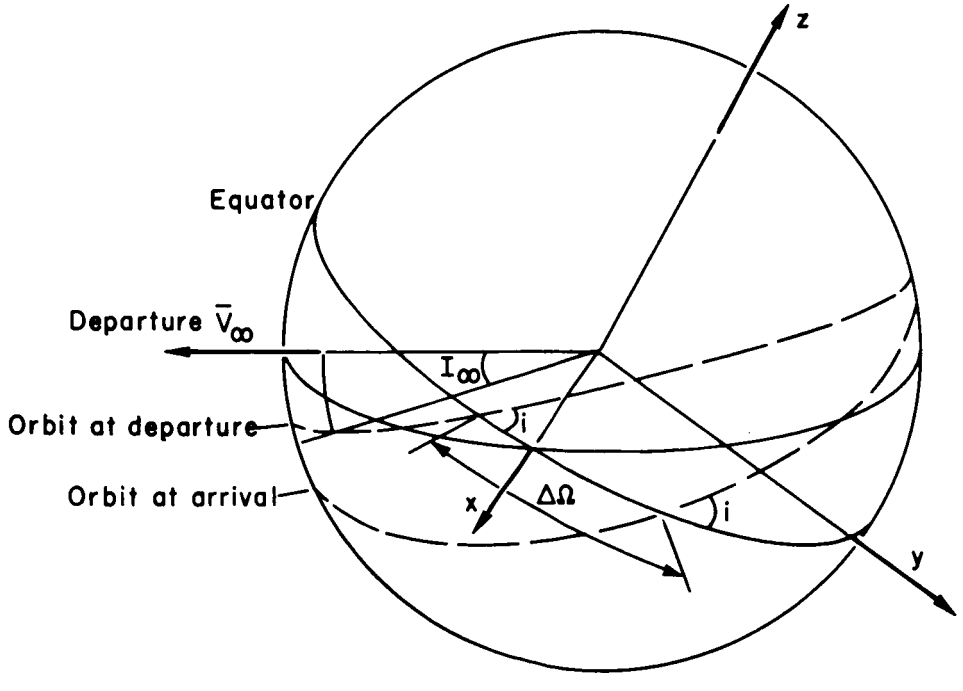

Figure 2.- Orbit geometry at planet departure.

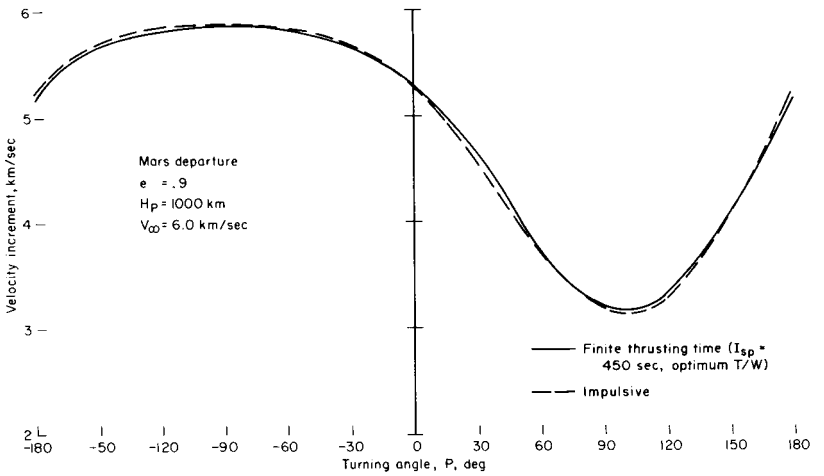

Figure 3.- Effect of finite thrusting time on turning angle.

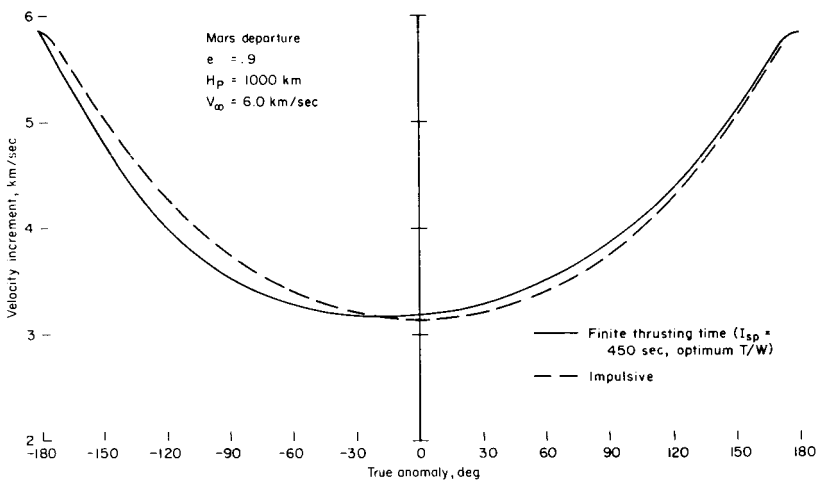

Figure 4.- Effect of finite thrusting time on ignition true anomaly.

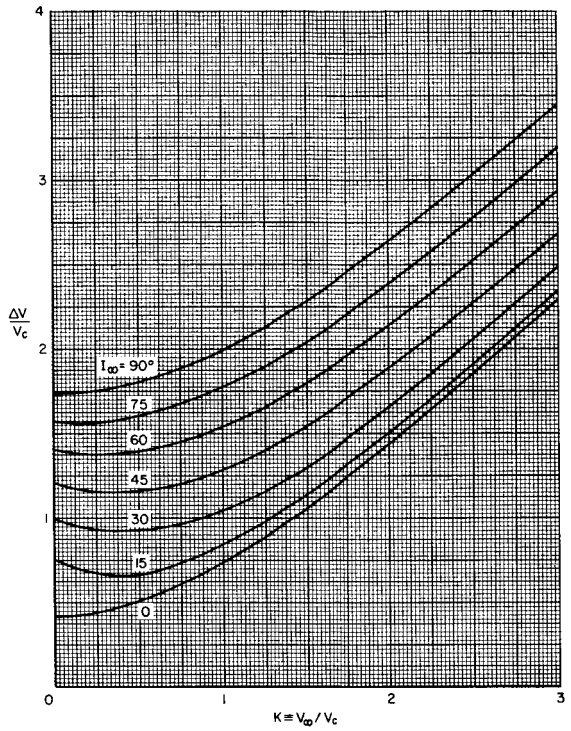

Figure 5.- Optimum one-impulse transfers.

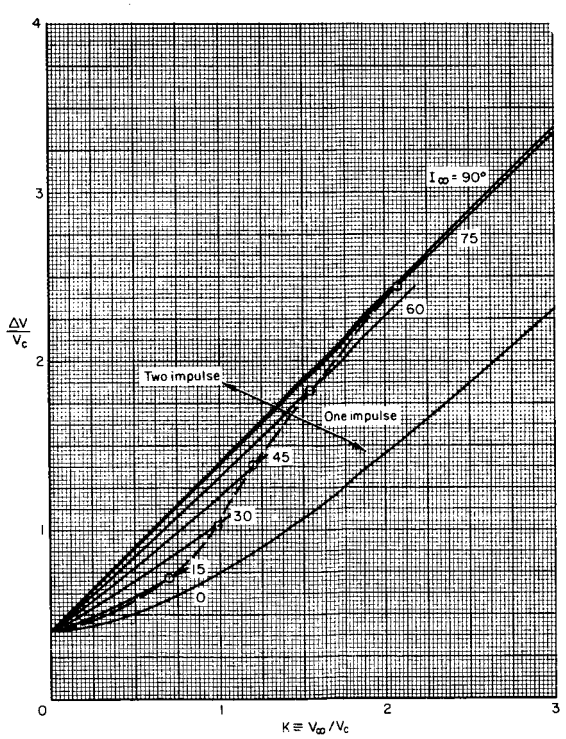

Figure 6.- Region of optimum two-impulse transfers.

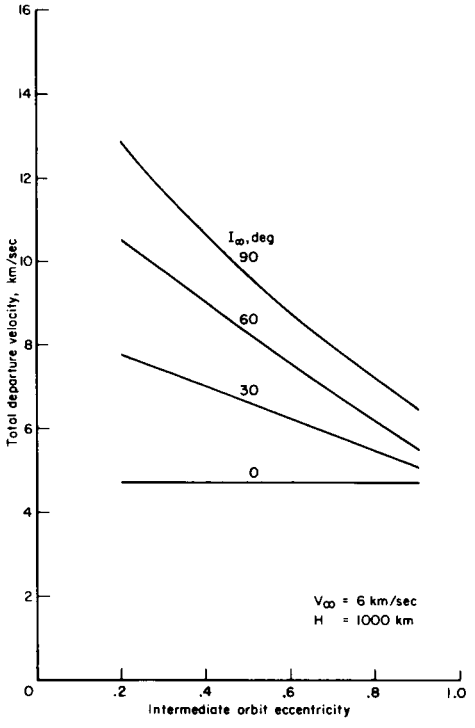

(a) From Earth orbit.

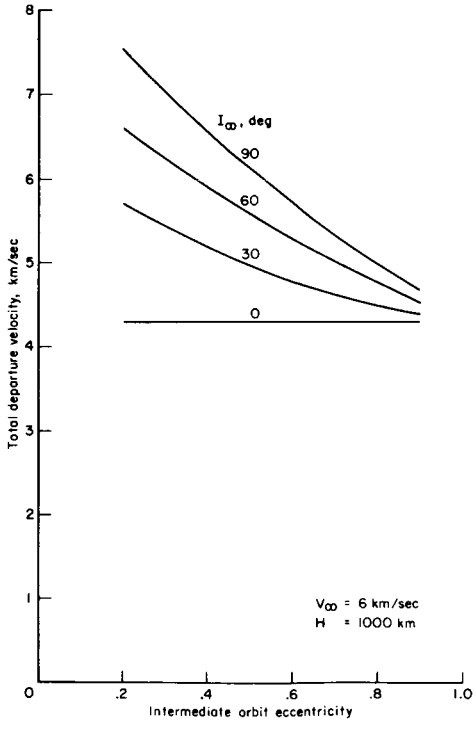

(b) From Mars orbit.

Figure 7.- Effect of eccentricity on three-impulse transfers.

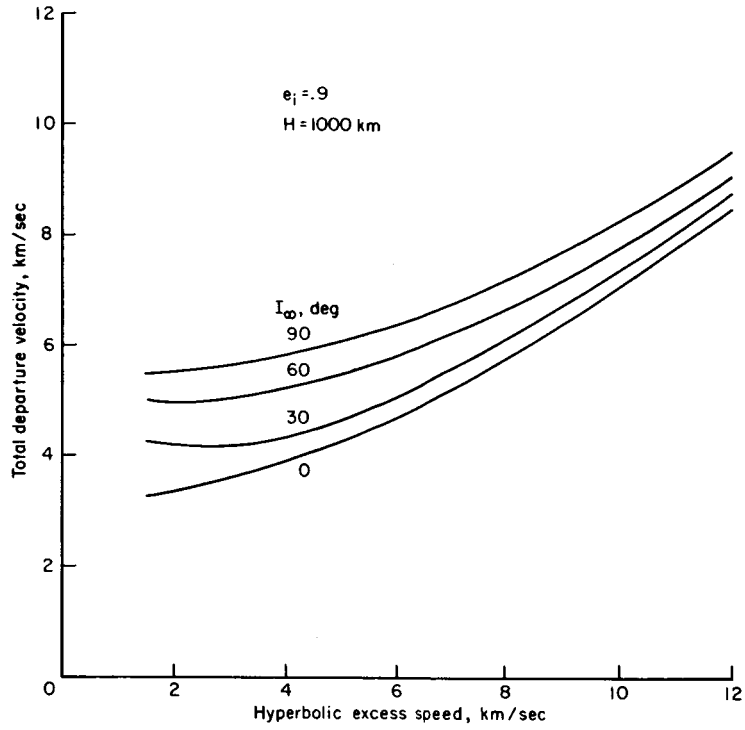

(a) From Earth orbit.

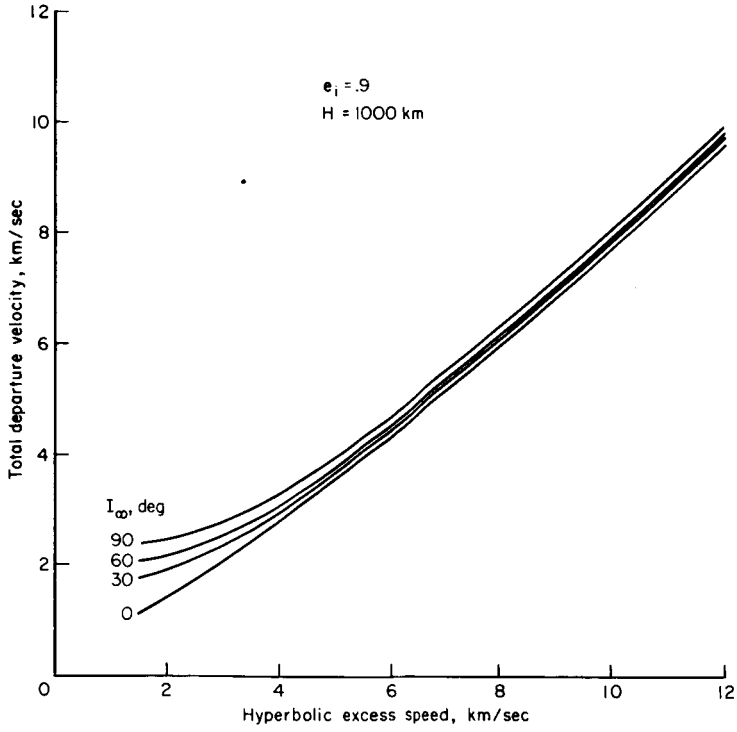

(b) From Mars orbit.

Figure 8.- Effect of excess speed on three-impulse transfers.

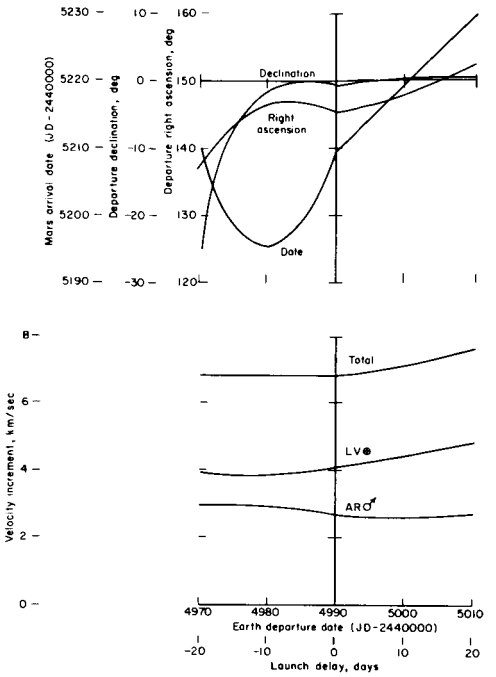

(a) 1982 inbound swingby.

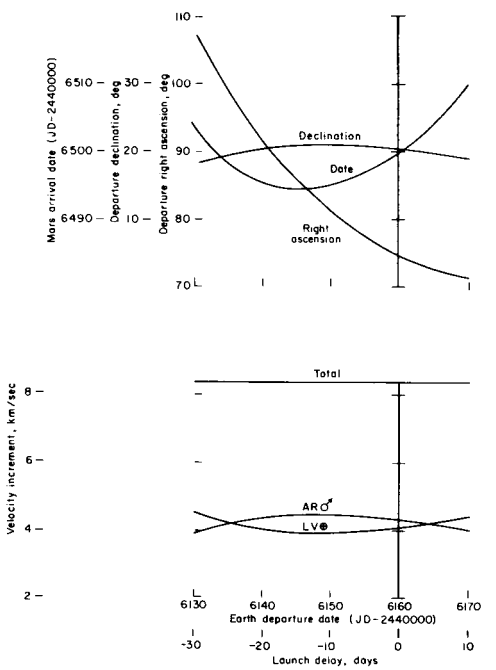

(b) 1986 outbound swingby.

Figure 9.- Outbound leg trajectory characteristics.

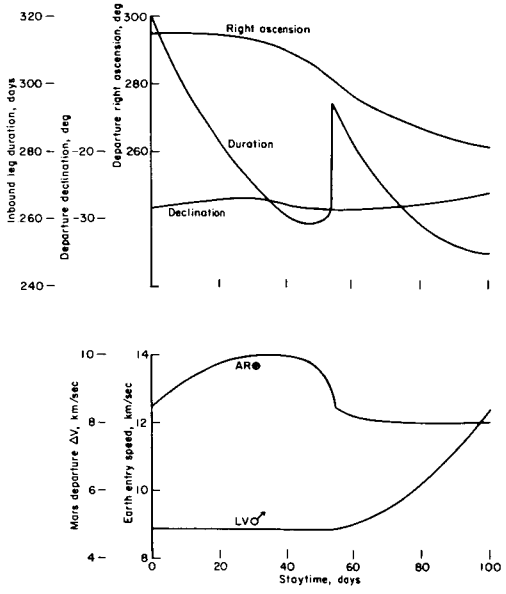

(a) 1982 inbound swingby (Mars arrival date = 244 5210).

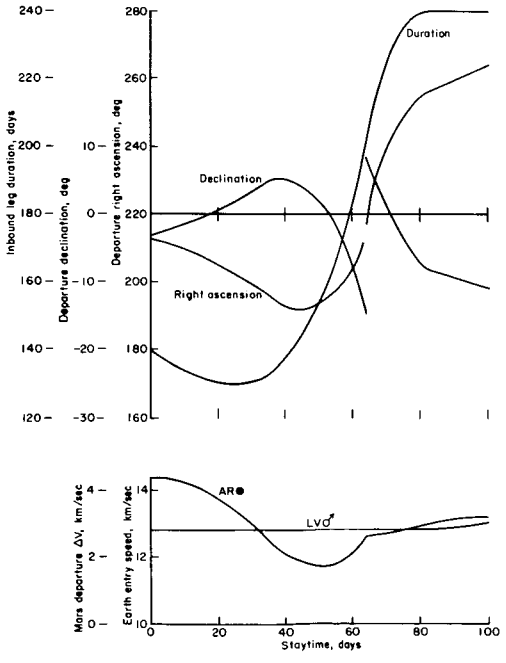

(b) 1986 outbound swingby (Mars arrival date = 244 6500).

Figure 10.- Inbound leg trajectory characteristics.

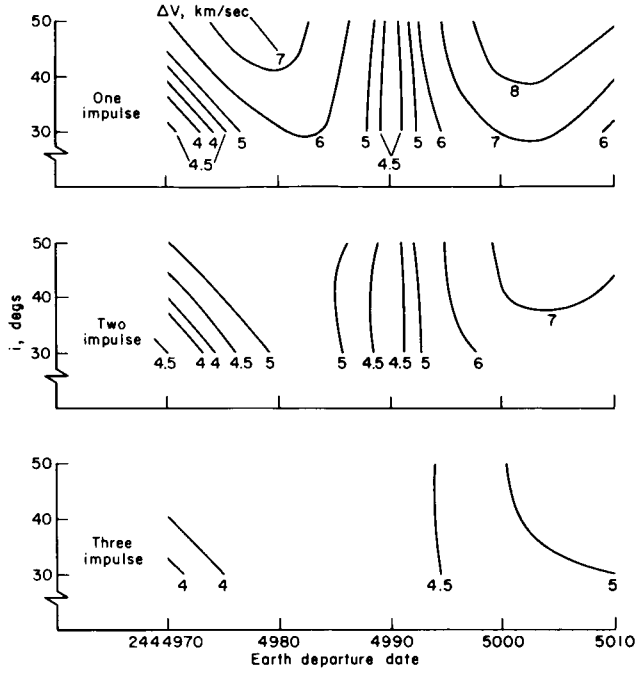

(a) Southern injection.

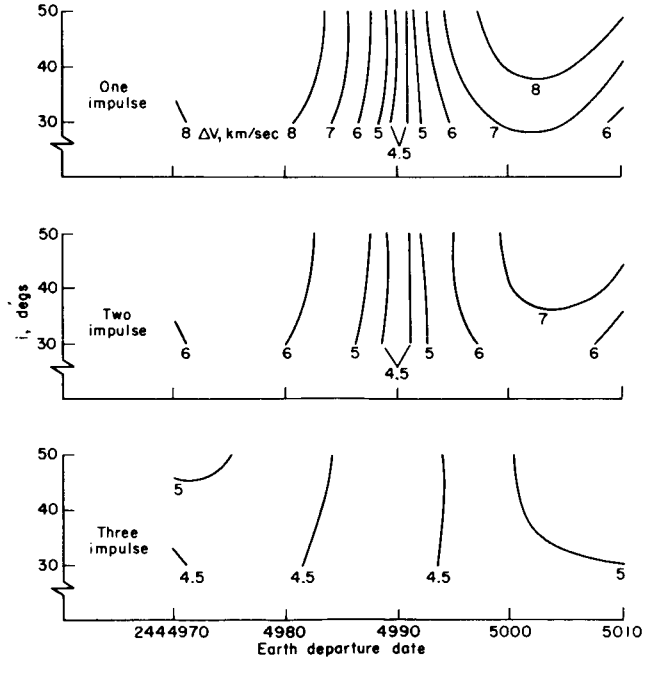

(b) Northern injection.

Figure 11.- Earth departure ΔV contours, 1982 inbound swingby.

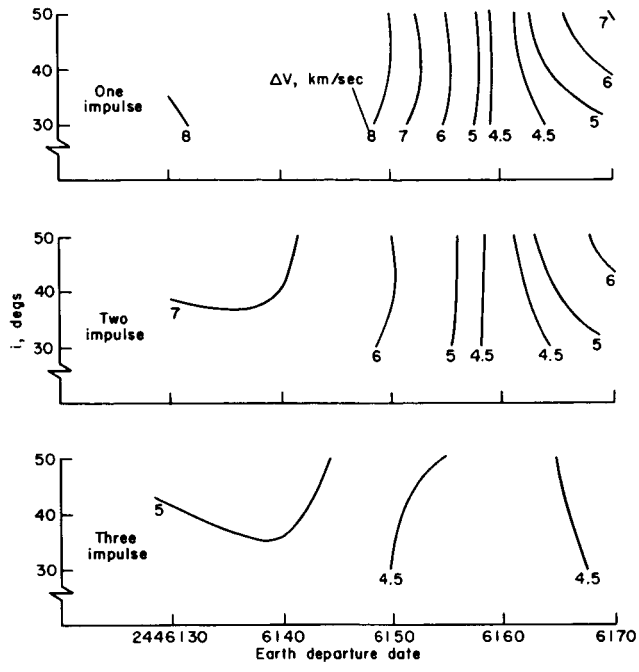

(a) Southern injection.

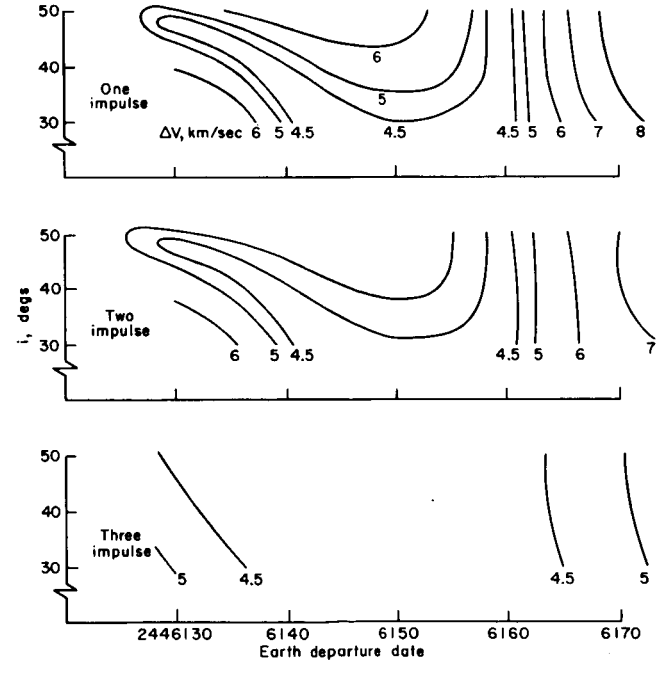

(b) Northern injection.

Figure 12.- Earth departure ΔV contours, 1986 outbound swingby.

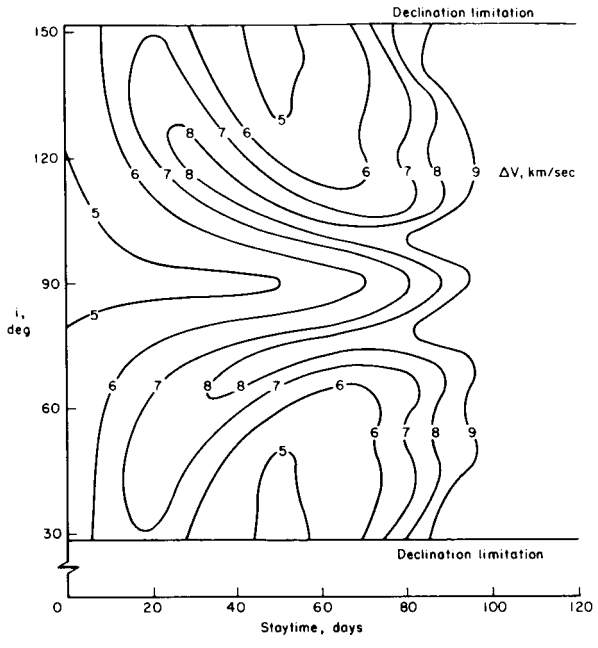

(a) Southern insertion, one impulse.

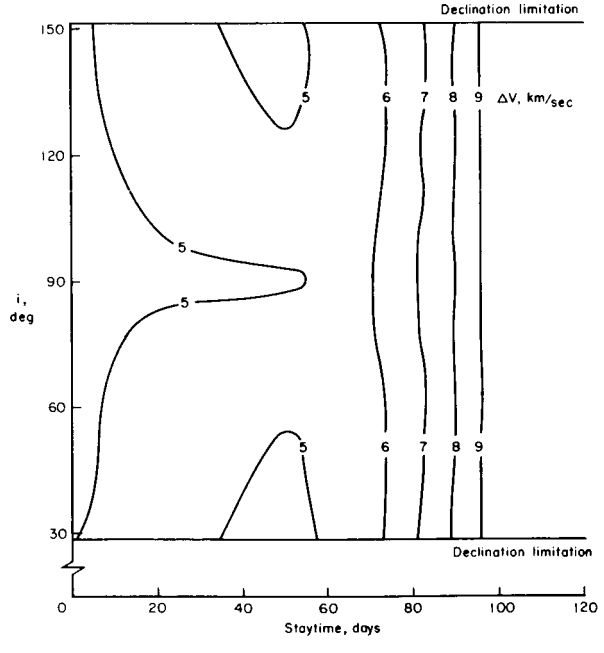

(b) Southern insertion, three impulse.

Figure 13.- Mars departure ΔV contours, 1982 inbound swingby.

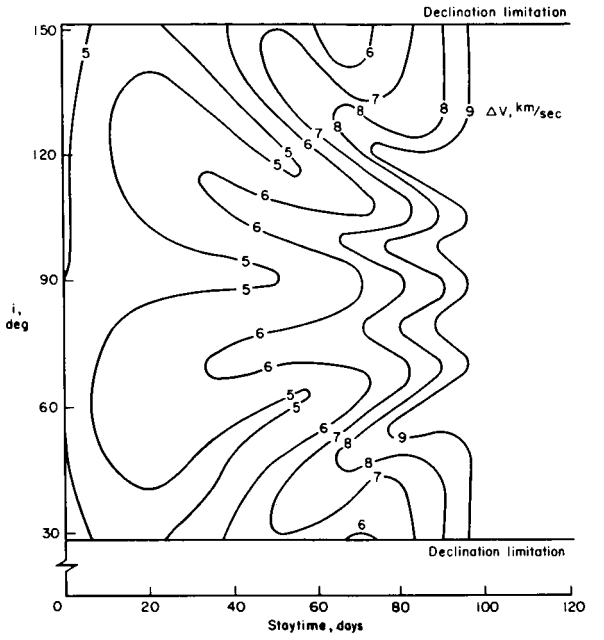

(c) Northern insertion, one impulse.

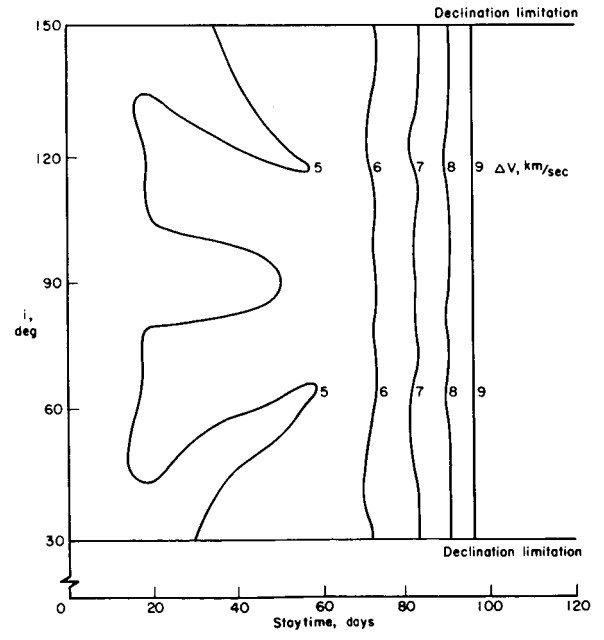

(d) Northern insertion, three impulse.

Figure 13.- Concluded.

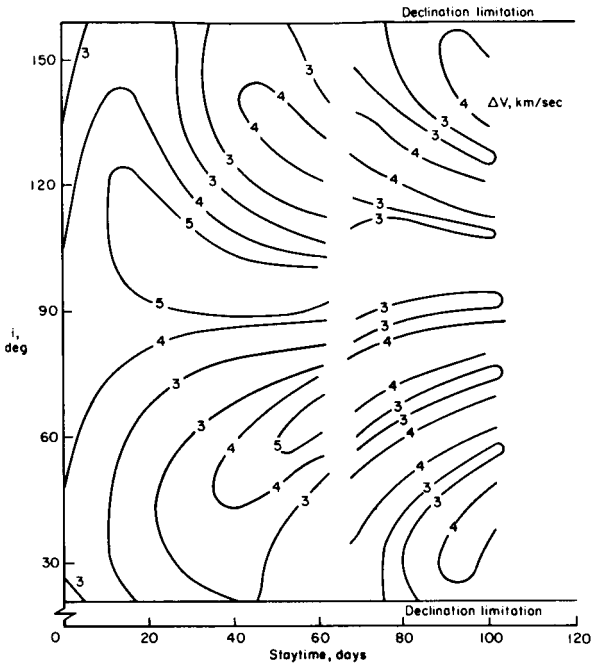

(a) Southern insertion, one impulse.

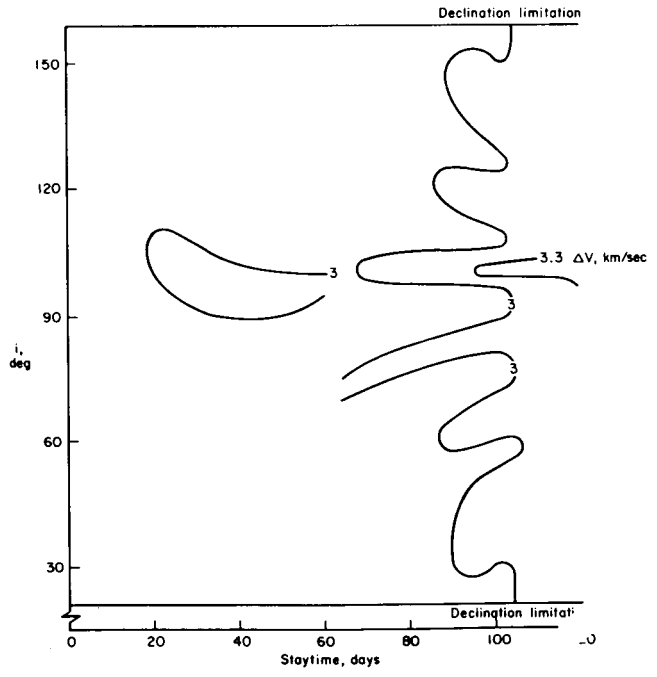

(b) Southern insertion, three impulse.

Figure 14.- Mars departure ΔV contours, 1986 outbound swingby.

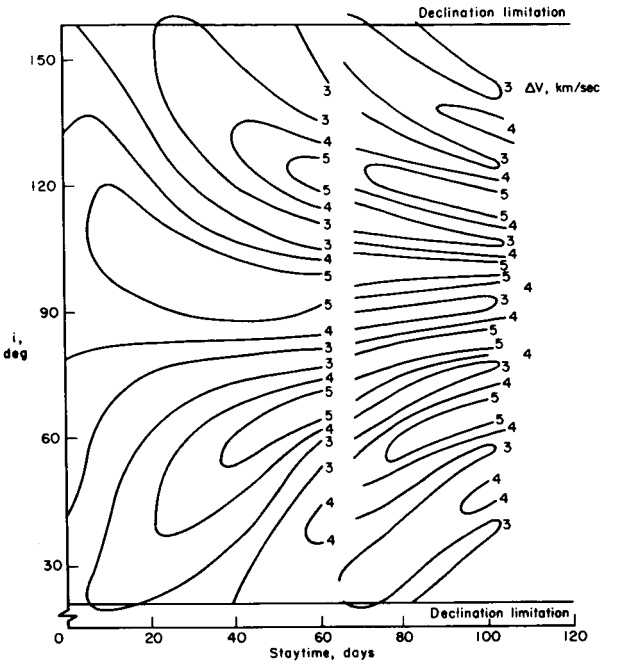

(c) Northern insertion, one impulse.

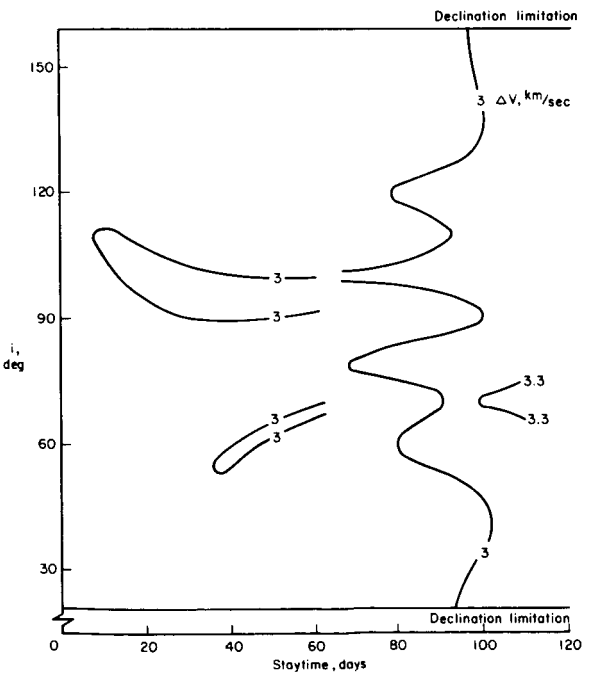

(d) Northern insertion, three impulse.

Figure 14.- Concluded.

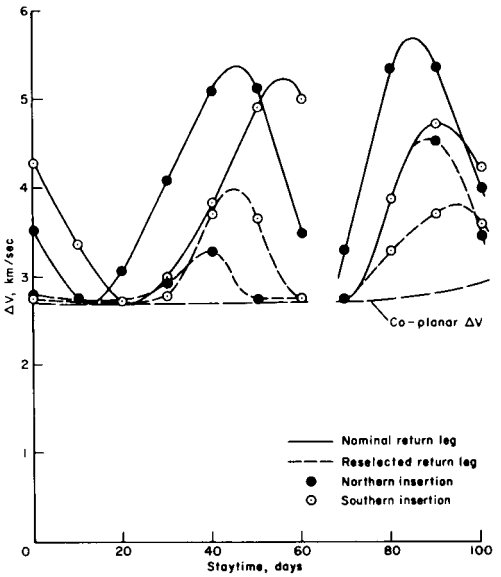

Figure 15.- Effect of direct leg reselection; 1986 outbound swingby, i = 60°, one impulse.

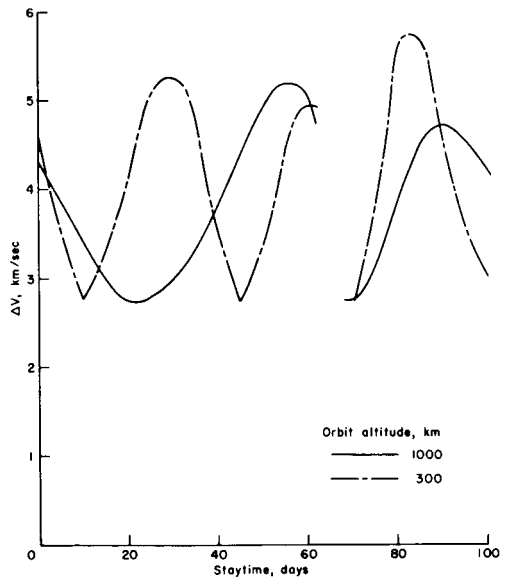

Figure 16.- Effect of orbit altitude on ΔV for one impulse; 1986 outbound swingby, southern insertion, i = 60°.

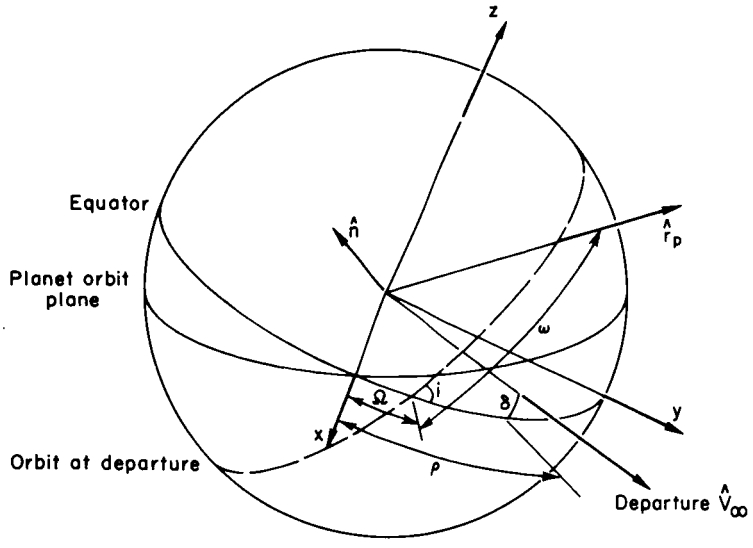

Figure 17.- Orbit geometry.

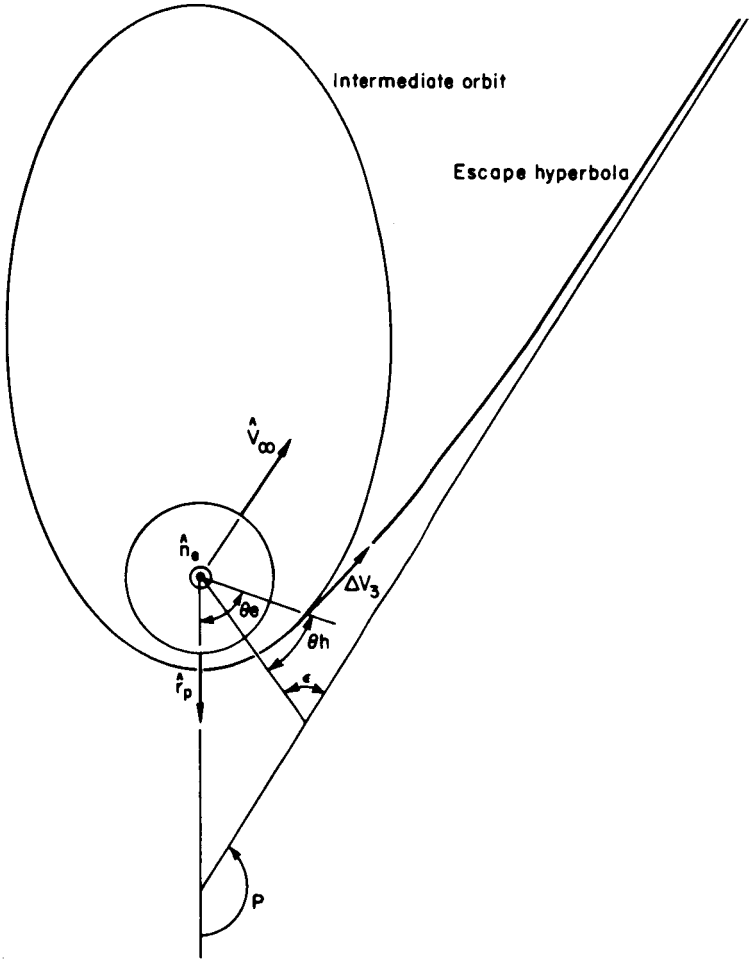

Figure 18.- Escape geometry.

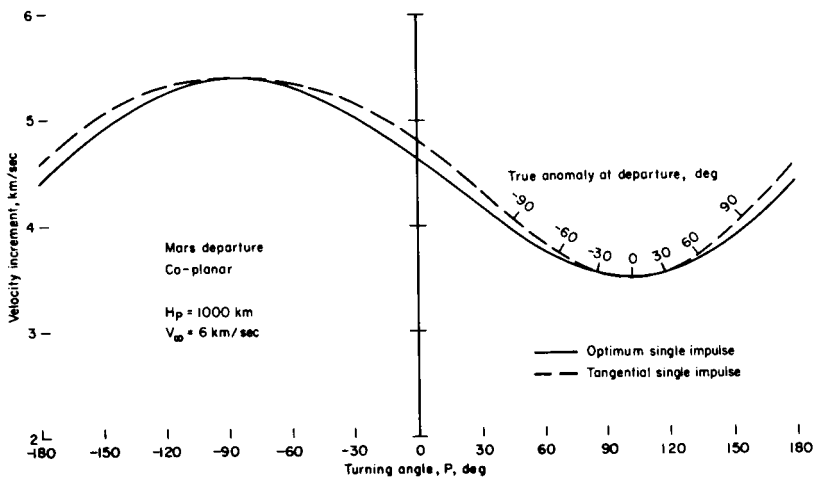

Figure 19.- Comparison of optimum and tangential single impulse departures; eccentricity = 0.6.

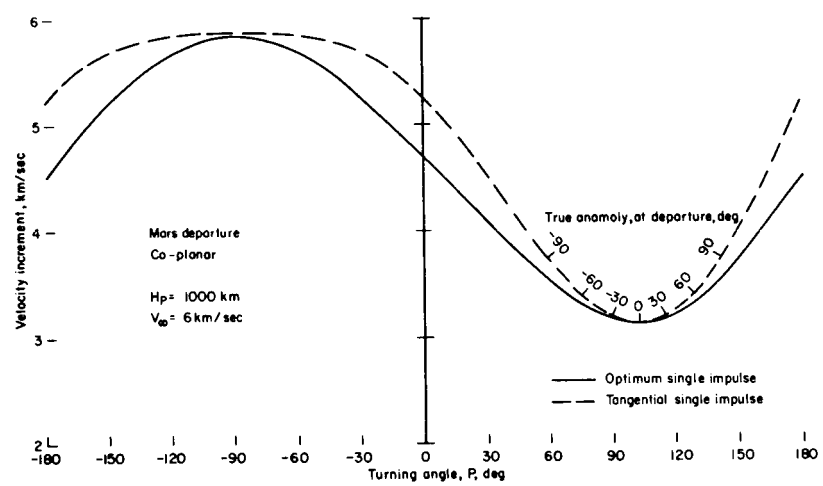

Figure 20.- Comparison of optimum and tangential single impulse departures; eccentricity = 0.9.

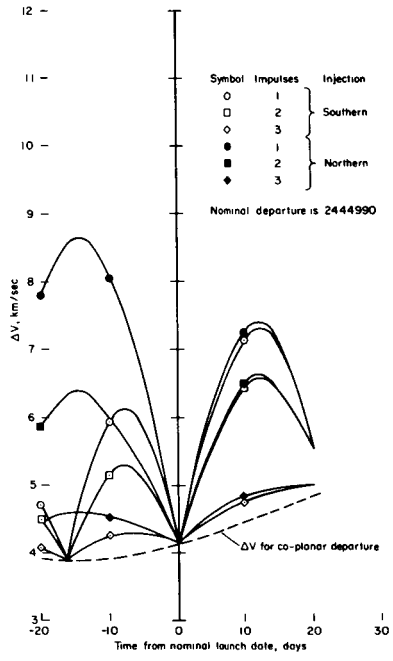

(a) i = 30°

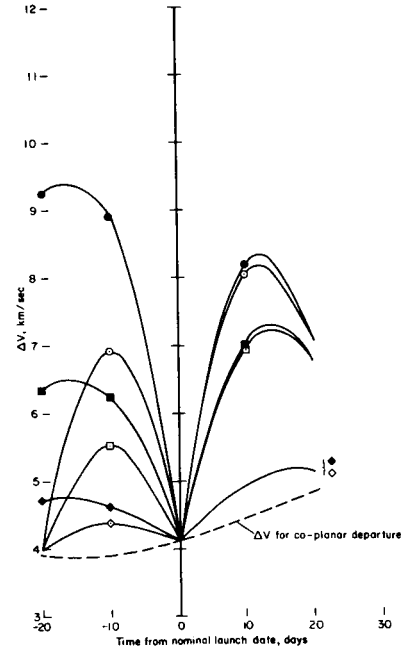

(b) i = 40°

Figure 21.- Earth depart total ΔV requirements, 1982 inbound swingby.

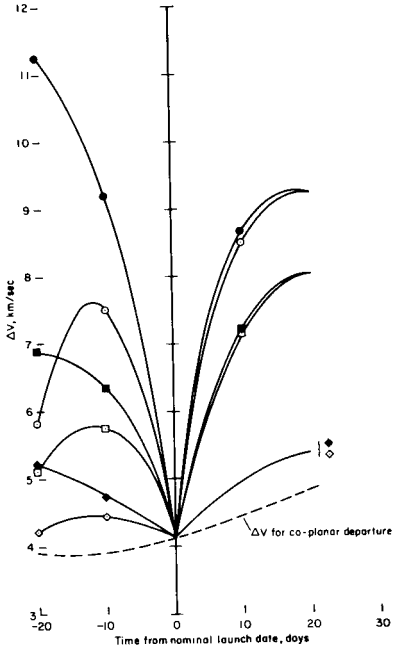

(c) $i = 50^{\circ}$

Figure 21.- Concluded.

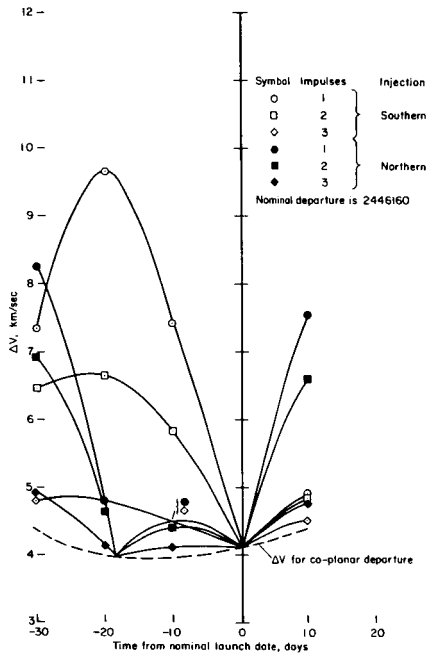

(a) i = 30°

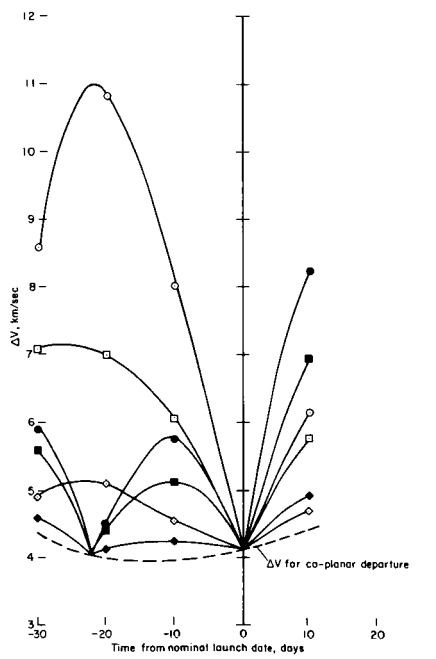

(b) i = 40°

Figure 22.- Earth depart total ΔV requirements, 1986 outbound swingby.

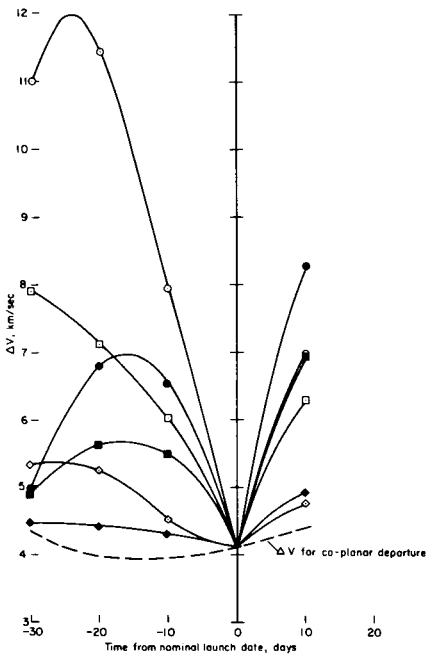

(c) $i = 50^{\circ}$

Figure 22.- Concluded.

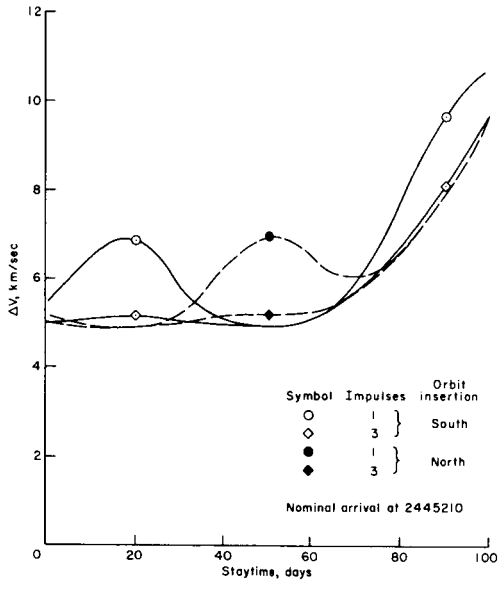

(a) i = 30.0

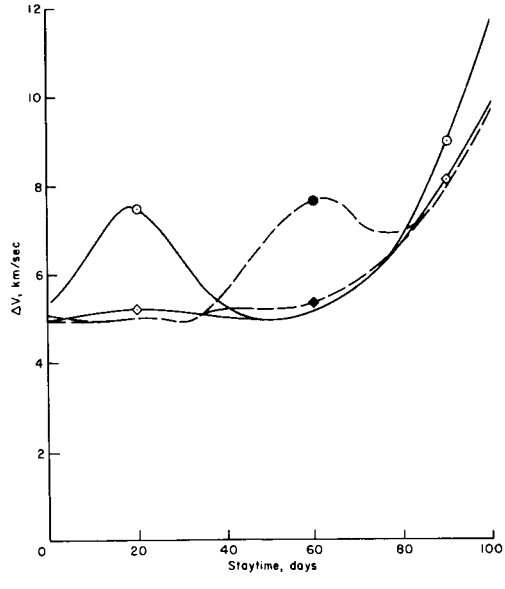

(b) i = 40.0

Figure 23.- Mars departure ΔV requirements; 1982 Mars mission, inbound Venus swingby.

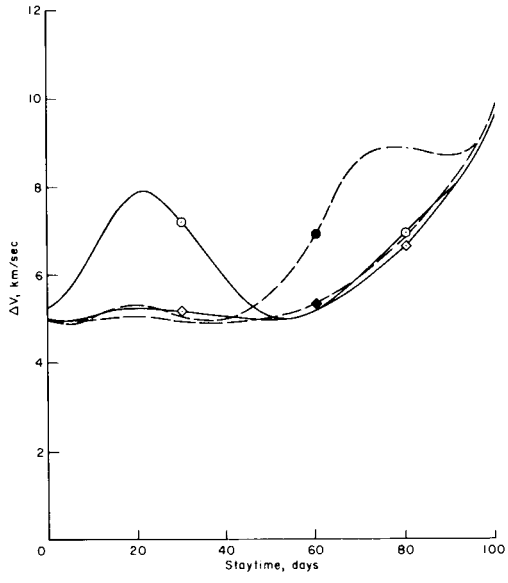

(c) i = 50.0

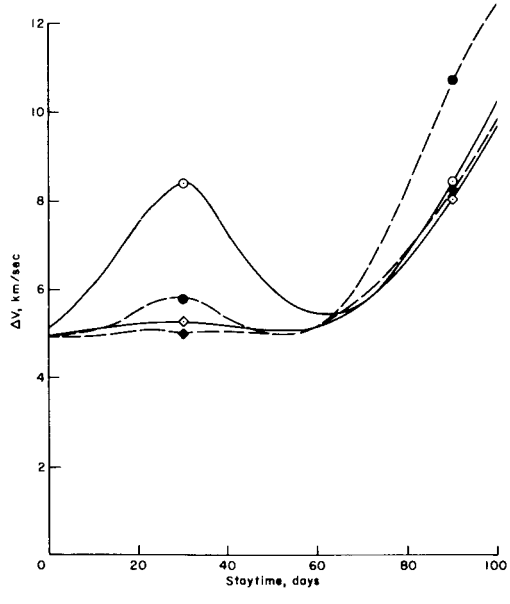

(d) i = 60.0

Figure 23.- Continued.

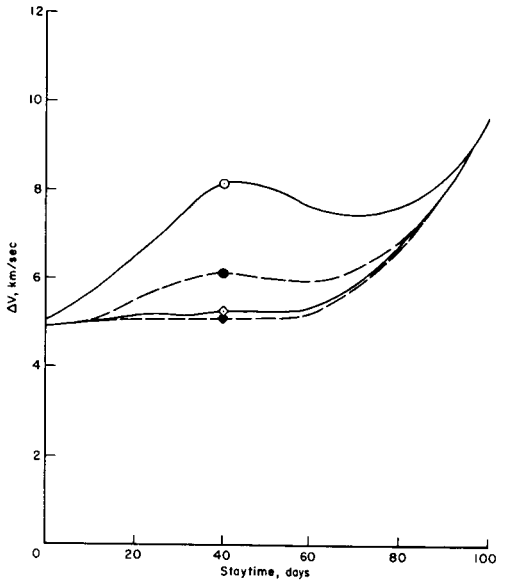

(e) i = 70.0

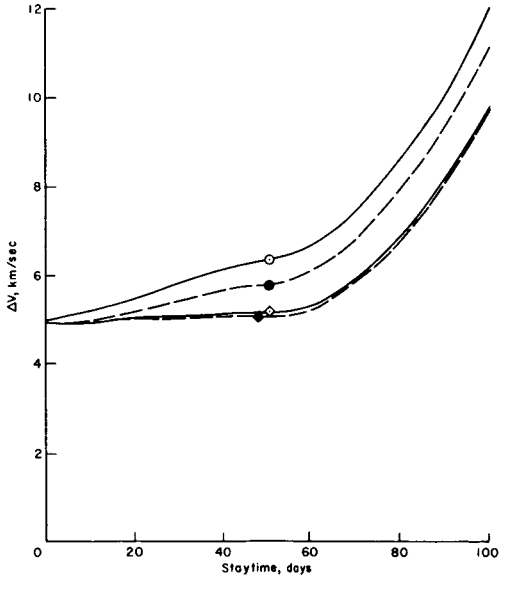

(f) i = 80.0

Figure 23.- Continued.

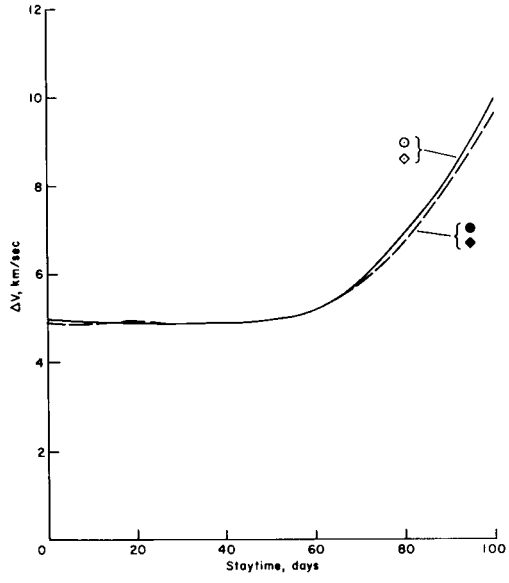

(g) i = 90.0

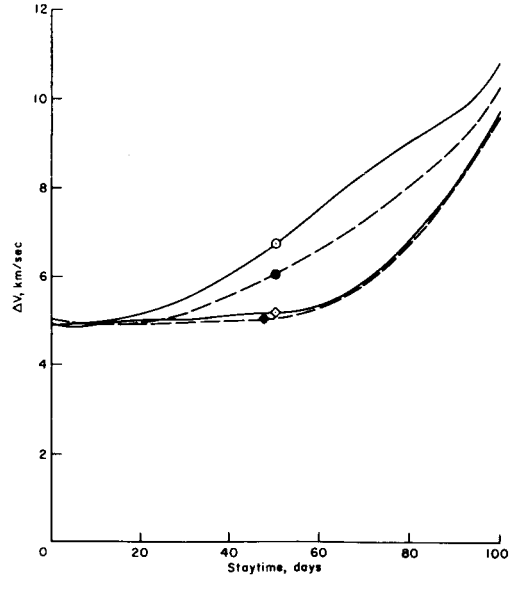

(h) i = 100.0

Figure 23.- Continued.

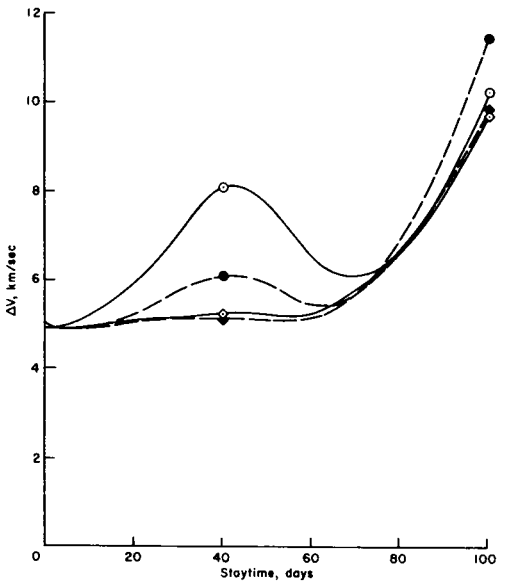

(i) i = 110.0

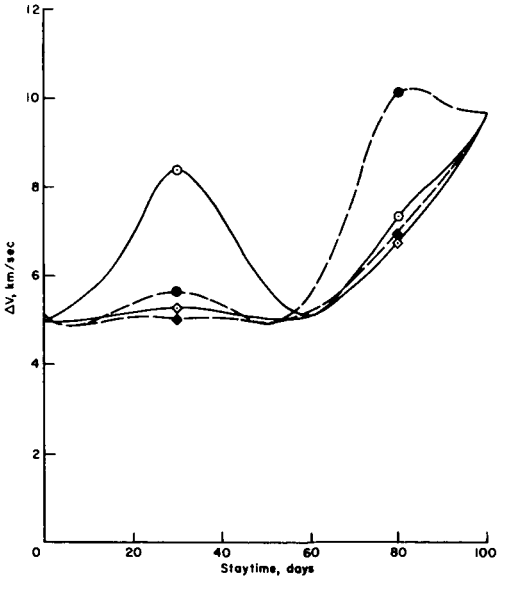

(j) i = 120.0

Figure 23.- Continued.

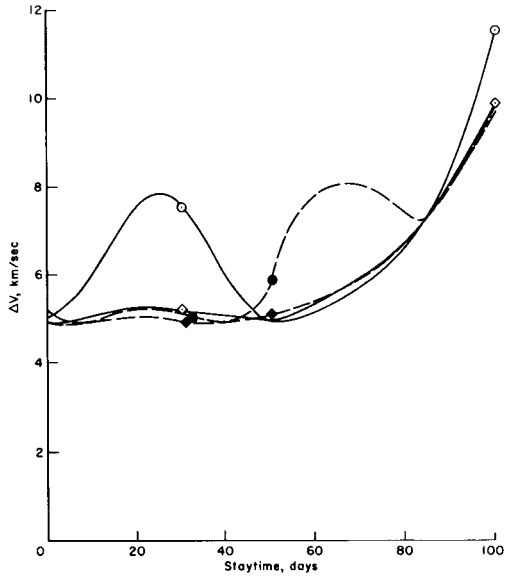

(k) i = 130.0

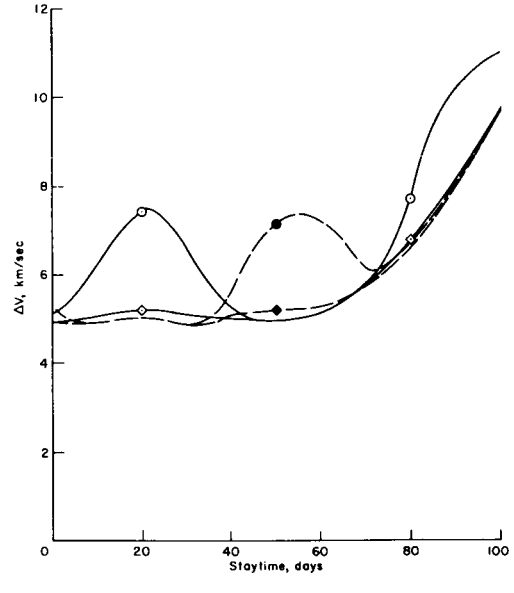

(l) i - 140.0

Figure 23.- Continued.

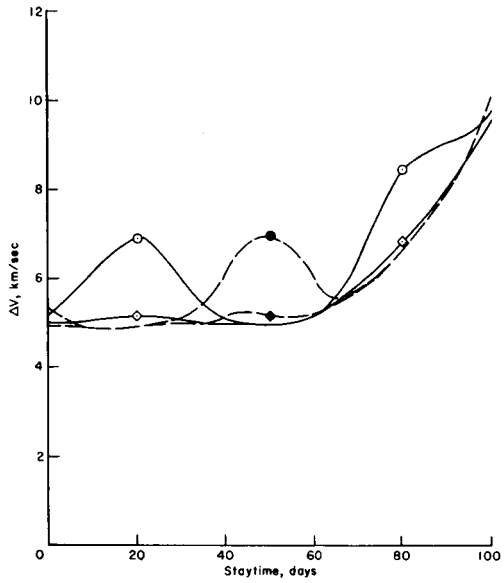

(m) i = 150.0

Figure 23.- Concluded.

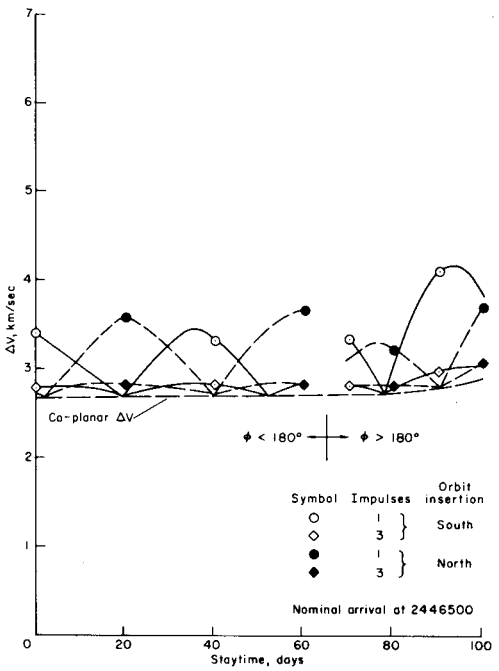

(a) i = 30.0

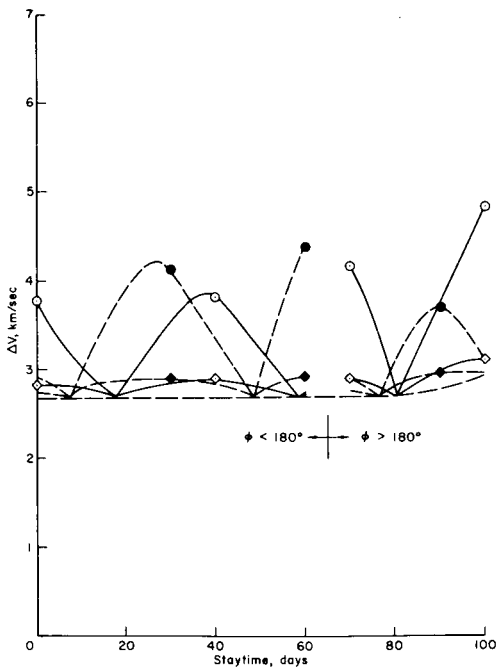

(b) i = 40.0

Figure 24.- Mars departure ΔV requirements, 1986 Mars mission.

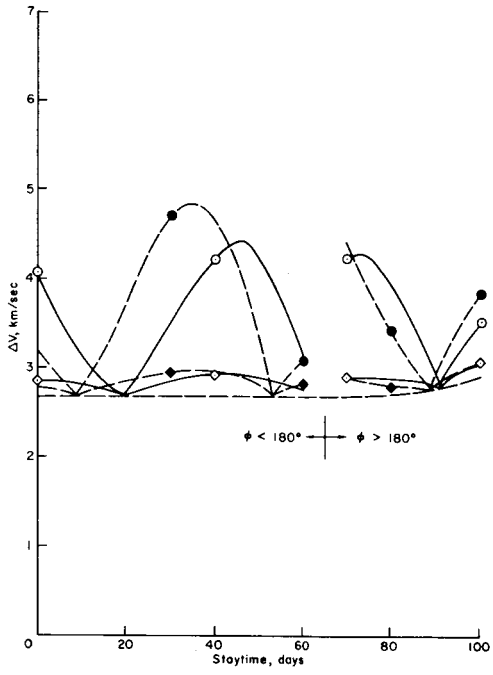

(c) i = 50.0

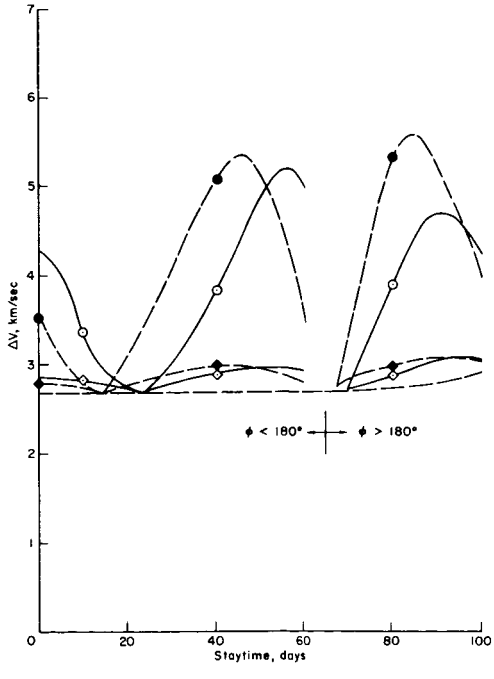

(d) i = 60.0

Figure 24.- Continued.

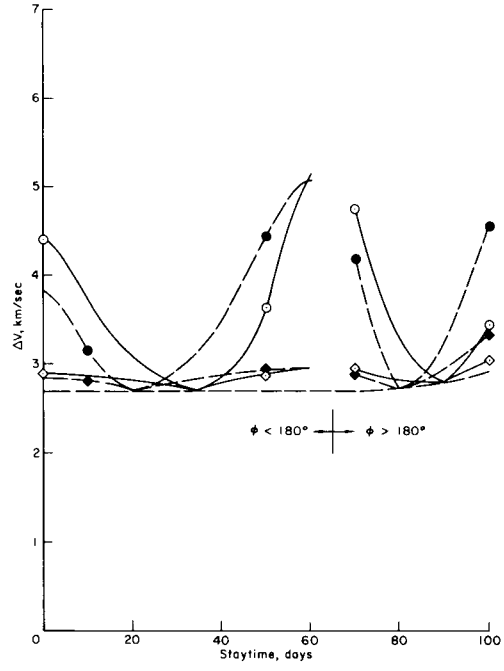

(e) i = 70.0

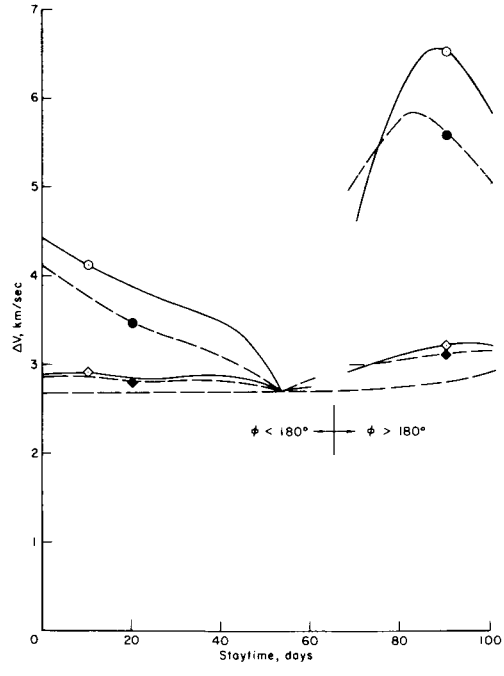

(f) i = 80.0

Figure 24.- Continued.

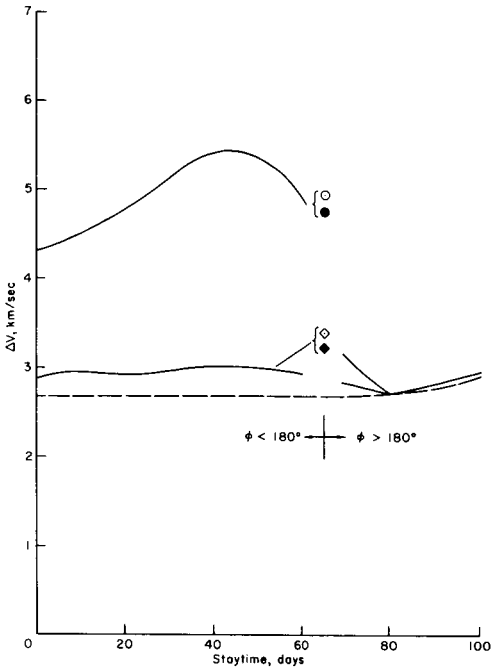

(g) i = 90.0

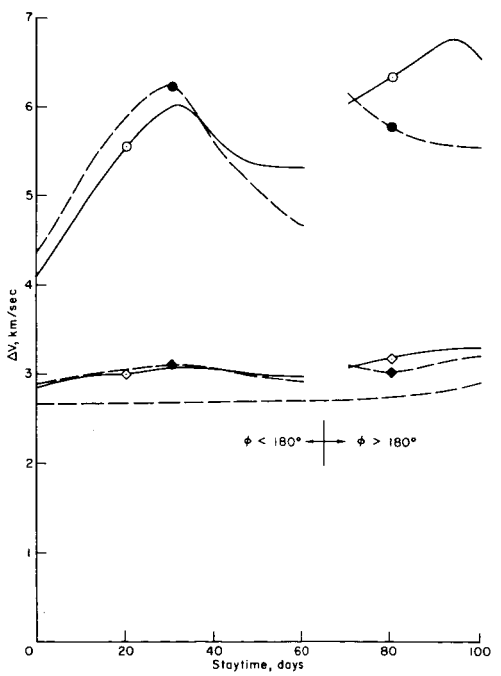

(h) i = 100.0

Figure 24.- Continued.

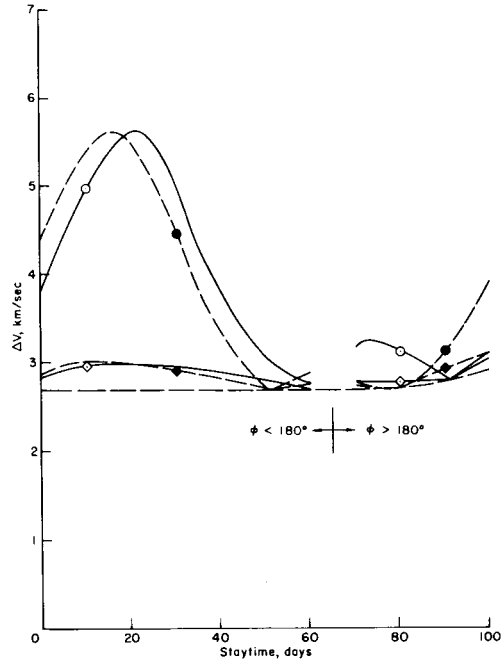

(i) i = 110.0

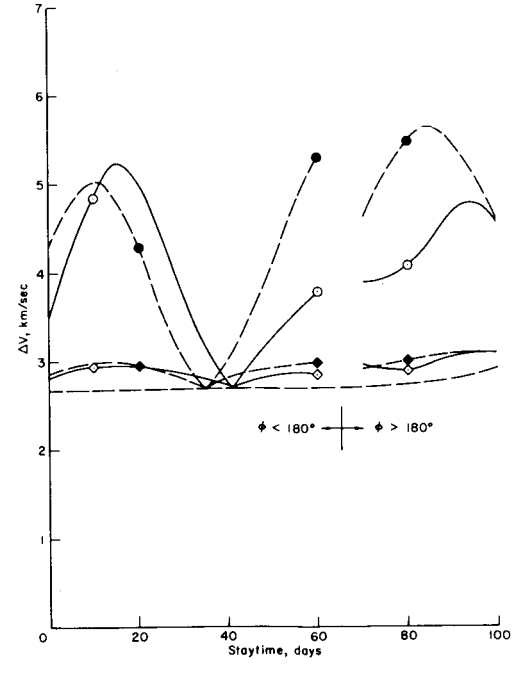

(j) i = 120.0

Figure 24.- Continued.

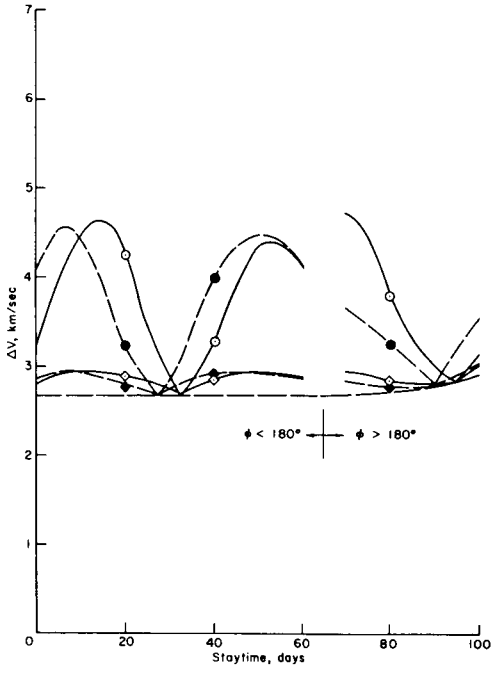

(k) i = 130.0

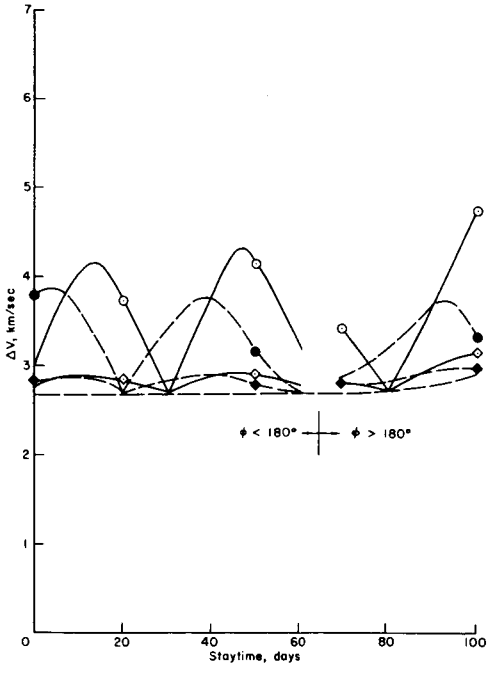

(l) i = 140.0

Figure 24.- Continued.

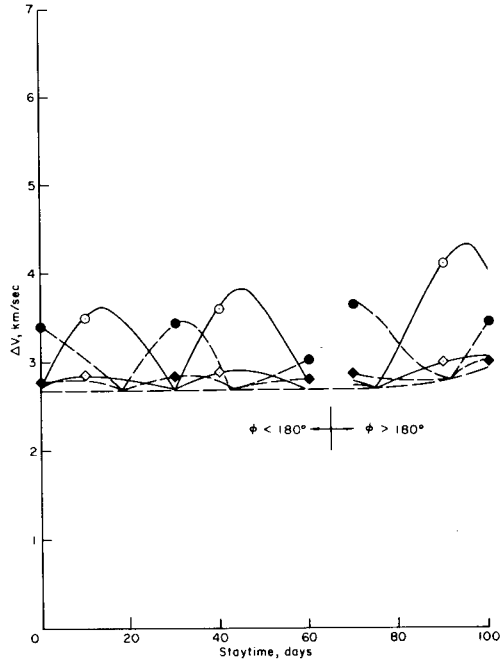

(m) i = 150.0

Figure 24.- Concluded.

NASA-Langley, 1968 —— 30